Explicit Verlet time–integration for a Nitsche–based approximation of elastodynamic contact problems

Franz Chouly, Yves Renard

Explicit Verlet time–integration for a Nitsche–based approximation of elastodynamic contact problems

Franz Chouly * Yves Renard †

June 13, 2018

Abstract

The aim of the present paper is to study theoretically and numerically the Verlet scheme for the explicit time–integration of elastodynamic problems with a contact condition approximated by Nitsche's method. This is a continuation of papers [11, 12] where some implicit schemes (theta–scheme, Newmark and a new hybrid scheme) were proposed and proved to be well-posed and stable under appropriate conditions. A theoretical study of stability is completed and illustrated with numerical experiments and comparison to other existing discretizations of contact problems.

Key words: unilateral contact, elastodynamics, Nitsche's method, explicit time–marching schemes, stability, explicit dynamics.
AMS Subject Classification: 65N12, 65N30, 74M15.

1 Introduction and problem setting

Explicit time–marching schemes for the dynamics of deformable solids with impact has already been the subject of an abundant literature (see, e.g., [15, 46, 56] for some recent contributions). They are appealing since they can be of easy implementation, fast and adapted to parallel architectures. Nevertheless, there still remains important difficulties to design robust explicit methods and to obtain reliable numerical simulations in this context (see, e.g., [51]).

A precursory method is the one developed by L.M. Taylor and D.P. Flanagan [52] in the framework of PRONTO3D software (see also the description in [29]). Nevertheless, the method is not fully explicit, except in a node–to–node contact approximation, in the sense that the contact pressure is computed in an iterative process on the whole contact surface. To mention some other of the most important contributions, we can say that a widely resumed theoretical work in dynamic impact problems is due to J.J. Moreau [35, 36] for the impact of rigid body systems. The (implicit) schemes proposed by J.J. Moreau have been extended quite naturally to the elasticity case through finite element semi–discretization in space (for instance in [54]) which transforms the continuous impact problem into a discrete one very close to a rigid body system. These discrete impact problems, governed by a so-called measure differential inclusion are notoriously ill-posed and of very low regularity.

*Laboratoire de Mathématiques de Besançon UMR6623, Université Bourgogne Franche Comté, CNRS; 16 route de Gray, 25030 Besançon Cedex, France. email: franz.chouly@univ-fcomte.fr

†ICJ UMR5208, LaMCoS UMR5259, Université de Lyon, INSA-Lyon, CNRS; F-69621, Villeurbanne, France. email: yves.renard@insa-lyon.fr

The ill-posedness can be (for the most part) fixed by the addition of an impact law with a restitution coefficient. As a matter of fact, standard schemes, such as the commonly used ones of Newmark's family [37], have an erratic behavior when they are applied to dynamic contact problems. This is mainly because they select a solution corresponding to an arbitrary (and potentially very large) restitution coefficient (see [30]). Alternatively, a valuable scheme in this context is that of L. Paoli and M. Schatzman [41, 42] who implicitly takes into account this restitution coefficient. However, the addition of a restitution coefficient can be considered as artificial in the context of deformable solids. This does not diminish the interest for the Paoli–Schatzman scheme which will be a point of comparison with our proposed approach. The implicit inclusion of a restitution coefficient has also been considered in [49] to develop a wide range of schemes based on a time discontinuous Galerkin framework.

As noticed in [30], even in the case where the continuous problem is well-posed (see, e.g., [19, 34] for well-posedness results), the ill-posed measure differential inclusion that results from finite element semi-discretization in space has an infinite number of solutions, depending on the choice of a restitution coefficient on each node of the contact boundary. Moreover, it is not possible to decide which solution is more suitable than other. Indeed, the two most remarkable solutions are, on the one hand, the one for a unitary restitution coefficient which ensures conserving energy but which causes very important spurious oscillations of the contact nodes and unexploitable contact stress, and, on the other hand, the solution for a vanishing restitution coefficient which ensures stability and a better approximation of the contact stress but is energy dissipative, while the continuous problem is not. This resulted in [30] to design the mass redistribution method (generalized in [26, 45]) which allows a compromise in this context, i.e. well-posedness of the space semi-discretized problem, conservation of the energy and an improved quality of the contact stress. However, and this is also the case for the Paoli–Schatzman scheme, it introduces a global problem to be solved (at least on the contact nodes) when an explicit time–marching scheme is used. In the same spirit, a time–marching scheme has been designed in [23] for dynamic fracture problems, in which the cohesive forces are treated implicitely, while an explicit scheme is used for the dynamics of interior nodes.

For explicit time–integration, primal formulations of contact conditions are better suited. Indeed, since no additional unknown such as a Lagrange multiplier are introduced, they allow to enforce the contact conditions at the previous time–step, instead of the current one, so that the contact term appears at the right-hand side and does not require global (and non-linear) solving. A first possibility is to penalize / regularize the contact conditions (see, e.g., [5, 31]): the resulting penalty method is simple to implement and only an inversion of the mass-matrix is needed at each time-step to solve the resulting fully discretized problem (and the scheme becomes fully explicit when the mass matrix is lumped). Nevertheless, the penalty method is not consistent and the choice of the penalty parameter remains a difficulty (see, e.g., [22]). The alternative we explore in this paper is a Nitsche treatment of contact conditions, which is still a primal method, with the same advantages as penalty, but that remains consistent with the original problem, and more robust with respect to the Nitsche parameter. Nitsche's method, originally designed to enforce weakly Dirichlet boundary conditions [38, 50], was adapted to unilateral contact in [9, 13] (see also [8] for an overview of recent results on this topic).

We studied previously in [11, 12] the behavior of Nitsche's method for contact in elastodynamics, when combined to various implicit time–marching schemes. Particularly, when applied to contact-impact in elastodynamics, Nitsche's method has the good property of leading to a well-posed semi–discrete problem in time (i.e., a system of Lipschitz differential equations) as it is shown in [11]. This feature is shared also by the penalty method and modified mass methods.

Moreover the symmetric variant of Nitsche's space semi-discretization conserves an augmented energy [11], as does the penalty method [28]. We studied as well theoretically the well-posedness, the stability and energy conservation properties of fully discrete schemes based on space semi-discretization with Nitsche's method combined with the theta–scheme, the Newmark scheme and a new Hybrid scheme. This study was illustrated with some numerical experiments.

The aim of this paper is to study mathematically and numerically the approximation of contact problems in elastodynamics by Nitsche's method combined with the explicit Verlet time–marching scheme. The choice of the Verlet scheme is motivated both by its simplicity and its attractive theoretical properties (symplecticity) [27]. We will also make comparisons with some of the existing methods mentioned above and with the approximation by penalized contact. The numerical comparison will be mainly performed on the one-dimensional problem introduced in [19] whose advantage is to present a known periodic solution and to make clear the occurrence of parasitic oscillations, the convergence and energy conservation properties. Comparisons for 2D and 3D problems will also be presented.

Let us introduce some useful notations. In what follows, bold letters like $\mathbf{u}, \mathbf{v}$, indicate vector or tensor valued quantities, while the capital ones (e.g., $\mathbf{V}, \mathbf{K} \ldots$) represent functional sets involving vector fields. As usual, we denote by $(H^s(.))^d$, $s \in \mathbb{R}, d = 1, 2, 3$ the Sobolev spaces in one, two or three space dimensions (see [1]). The usual scalar product of $(H^s(D))^d$ is denoted by $(\cdot, \cdot)_{s,D}$ and the corresponding norm is denoted by $\| \cdot \|_{s,D}$ - we keep the same notation when $d = 1$ or $d > 1$. The letter C stands for a generic constant, independent of the discretization parameters.

We consider an elastic body Ω in $\mathbb{R}^d$ with $d = 1, 2, 3$. Small strain assumptions are made (as well as plane strain when $d = 2$). The boundary $\partial\Omega$ of Ω is polygonal ($d = 2$) or polyhedral ($d = 3$). The normal unit outward vector on $\partial\Omega$ is denoted $\mathbf{n}$. We suppose that $\partial\Omega$ consists in three nonoverlapping parts Γ_D, Γ_N and the contact boundary Γ_C, with $\text{meas}(\Gamma_D) > 0$ and $\text{meas}(\Gamma_C) > 0$. In its initial stage, the body is in contact on Γ_C with a rigid foundation and we suppose that the unknown contact zone during deformation is included into Γ_C. The body is clamped on Γ_D for the sake of simplicity. It is subjected to volume forces $\mathbf{f}$ in Ω and to surface loads $\mathbf{g}$ on Γ_N.

We deal with the unilateral contact problem in linear elastodynamics during a period of time $[0, T)$ where $T > 0$ is the final time. We denote by $\Omega_T := (0, T) \times \Omega$ the time-space domain, and similarly $\Gamma_{DT} := (0, T) \times \Gamma_D$, $\Gamma_{NT} := (0, T) \times \Gamma_N$ and $\Gamma_{CT} := (0, T) \times \Gamma_C$. The problem then consists in finding the displacement field $\mathbf{u} : [0, T) \times \Omega \to \mathbb{R}^d$ verifying the equations and conditions (1)–(2):

$$\begin{aligned} \rho\ddot{\mathbf{u}} - \mathbf{div}\,\boldsymbol{\sigma}(\mathbf{u}) = \mathbf{f}, \quad \boldsymbol{\sigma}(\mathbf{u}) = \mathbf{A}\,\boldsymbol{\varepsilon}(\mathbf{u}) &\qquad \text{in } \Omega_T, \\ \mathbf{u} = \mathbf{0} &\qquad \text{on } \Gamma_{DT}, \\ \boldsymbol{\sigma}(\mathbf{u})\mathbf{n} = \mathbf{g} &\qquad \text{on } \Gamma_{NT}, \\ \mathbf{u}(0, \cdot) = \mathbf{u}_0 \quad \dot{\mathbf{u}}(0, \cdot) = \dot{\mathbf{u}}_0 &\qquad \text{in } \Omega, \end{aligned} \tag{1}$$

where the notation $\dot{\mathbf{x}}$ is used for the time-derivative of a vector field $\mathbf{x}$ on Ω_T, so that $\dot{\mathbf{u}}$ is the velocity of the elastic body and $\ddot{\mathbf{u}}$ its acceleration; $\mathbf{u}_0$ and $\dot{\mathbf{u}}_0$ are initial displacement and velocity. The density of the elastic material is denoted by ρ, and is supposed to be a constant to simplify the presentation (this is not restrictive and the results can be extended straightforwardly for a variable density). The notation $\boldsymbol{\sigma} = (\sigma_{ij})$, $1 \le i, j \le d$, stands for the stress tensor field and **div** denotes the divergence operator of tensor valued functions. The notation $\boldsymbol{\varepsilon}(\mathbf{v}) = (\boldsymbol{\nabla}\mathbf{v} + \boldsymbol{\nabla}\mathbf{v}^T)/2$ represents the linearized strain tensor field and $\mathbf{A}$ is the fourth order symmetric elasticity tensor

having the usual uniform ellipticity and boundedness property. For any displacement field $\mathbf{v}$ and for any density of surface forces $\boldsymbol{\sigma}(\mathbf{v})\mathbf{n}$ defined on $\partial\Omega$ we adopt the following notation

$$\mathbf{v} = v_n\mathbf{n} + \mathbf{v_t} \quad \text{and} \quad \boldsymbol{\sigma}(\mathbf{v})\mathbf{n} = \sigma_n(\mathbf{v})\mathbf{n} + \boldsymbol{\sigma_t}(\mathbf{v}),$$

where $\mathbf{v_t}$ (resp. $\boldsymbol{\sigma_t}(\mathbf{v})$) is the tangential component of $\mathbf{v}$ (resp. $\boldsymbol{\sigma}(\mathbf{v})\mathbf{n}$). The conditions describing unilateral contact without friction on Γ_{CT} are:

$$u_n \leq 0 \quad \sigma_n(\mathbf{u}) \leq 0 \quad \sigma_n(\mathbf{u})\, u_n = 0 \quad \boldsymbol{\sigma_t}(\mathbf{u}) = \mathbf{0}. \tag{2}$$

Note additionally that the initial displacement $\mathbf{u}_0$ should satisfy the compatibility condition $u_{0n} \leq 0$ on Γ_C.

To our knowledge, the well-posedness of Problem (1)–(2) is still an open issue. The few available existence results concern simplified model problems involving the (scalar) wave equation with Signorini's conditions (see, e.g., [47, 48, 34, 32, 18]) or thin structures like membranes, beams (see [2]) or plates (see [44]). Even in these simplified cases, obtaining uniqueness and energy conservation still involves difficulties in 2D or 3D. For a review on some of these results, one can refer to the book [24].

We introduce the Hilbert space

$$\mathbf{V} \;:=\; \left\{\mathbf{v} \in \left(H^1(\Omega)\right)^d \;:\, \mathbf{v} = \mathbf{0} \text{ on } \Gamma_D\right\},$$

and the following forms:

$$a(\mathbf{u},\mathbf{v}) := \int_\Omega \boldsymbol{\sigma}(\mathbf{u}) : \boldsymbol{\varepsilon}(\mathbf{v})\; d\Omega, \qquad L(t)(\mathbf{v}) := \int_\Omega \mathbf{f}(t)\cdot\mathbf{v}\; d\Omega + \int_{\Gamma_N} \mathbf{g}(t)\cdot\mathbf{v}\; d\Gamma,$$

for any $\mathbf{u}$ and $\mathbf{v}$ in $\mathbf{V}$, for all $t \in [0,T)$. The (total) mechanical energy associated with the solution $\mathbf{u}$ of the dynamic contact problem (1)–(2) is:

$$E(t) := \frac{1}{2}\rho\|\dot{\mathbf{u}}(t)\|^2_{0,\Omega} + \frac{1}{2}a(\mathbf{u}(t),\mathbf{u}(t)), \quad \forall t \in [0,T].$$

Let us take $t \in [0,T]$. Formally, we get from (1), after multiplication by $\dot{\mathbf{u}}(t)$, integration by parts, with the boundary conditions on Γ_{DT}, Γ_{NT} and the absence of friction:

$$\underbrace{\int_\Omega \ddot{\mathbf{u}}(t)\cdot\dot{\mathbf{u}}(t)\; d\Omega + \int_\Omega \boldsymbol{\sigma}(\mathbf{u}(t)) : \boldsymbol{\varepsilon}(\dot{\mathbf{u}}(t))\; d\Omega}_{\frac{d}{dt}E(t)} - \int_{\Gamma_C} \sigma_n(\mathbf{u}(t))\dot{u}_n(t)\; d\Gamma = L(t)(\dot{\mathbf{u}}(t)).$$

Moreover, with the persistency condition $\sigma_n(\mathbf{u}(t))\dot{u}_n(t) = 0$ (see, e.g., [33, 4, 28]) we end up with:

$$\frac{d}{dt}E(t) = L(t)(\dot{\mathbf{u}}(t)). \tag{3}$$

In particular, when L vanishes, we get energy conservation: $E(t) = E(0)$, for all $t \in [0,T]$. Note that in the 1D case (elastic bar), the energy conservation can be established rigorously, see [18, Lemma 2.5].

The rest of our paper is outlined as follows. In Section 2, the fully discrete formulation for dynamic contact with Nitsche and Verlet explicit time–integration is introduced. A stability analysis is carried out in Section 3. Numerical experiments are described in Section 4.

2 Discrete setting: Nitsche's method with Verlet scheme

We begin this section with preliminary notations and results. Then, we introduce our Nitsche-based finite element semi-discretization in space, and we recall its main properties of well-posedness and energy conservation. Finally we describe the fully discretized problem based on the Verlet explicit time–marching scheme.

2.1 Preliminary notations and results

We make use of the notation $[\cdot]_{\mathbb{R}^-}$, that stands for the projection onto $\mathbb{R}^-$ ($[x]_{\mathbb{R}^-} = \frac{1}{2}(x - |x|)$ for $x \in \mathbb{R}$). The notation $H(\cdot)$ will stand for the Heaviside function $H(x) = 1$ if $x > 0$, $\frac{1}{2}$ if $x = 0$, and 0 if $x < 0$, which satisfies $H(x) + H(-x) = 1, \forall x \in \mathbb{R}$. Moreover we will make use of the equality $H(-x)[x]_{\mathbb{R}^-} = [x]_{\mathbb{R}^-}, \quad \forall x \in \mathbb{R}$, and the following property of projection:

$$(y - x)([y]_{\mathbb{R}^-} - [x]_{\mathbb{R}^-}) \geq ([y]_{\mathbb{R}^-} - [x]_{\mathbb{R}^-})^2 \qquad \forall x, y \in \mathbb{R}. \tag{4}$$

Let $\mathbf{V}^h \subset \mathbf{V}$ be a family of finite dimensional vector spaces (see [14]) indexed by h coming from a family $\mathcal{T}^h$ of triangulations of the domain Ω ($h = \max_{K \in \mathcal{T}^h} h_K$ where h_K is the diameter of the triangle K). The family of triangulations is supposed:

- regular, i.e., there exists $\sigma > 0$ such that $\forall K \in \mathcal{T}^h, h_K/\rho_K \leq \sigma$ where ρ_K denotes the radius of the inscribed ball in K,
- conformal to the subdivision of the boundary into Γ_D, Γ_N and Γ_C, which means that a face of an element $K \in \mathcal{T}^h$ is not allowed to have simultaneous non-empty intersection with more than one part of the subdivision,
- quasi-uniform, i.e., there exists $c > 0$, such that, $\forall h > 0,\ \forall K \in \mathcal{T}^h,\ h_K \geq ch$.

To fix ideas, we choose a standard Lagrange finite element method of degree k with $k = 1$ or $k = 2$, i.e.:

$$\mathbf{V}^h = \left\{ \mathbf{v}^h \in (\mathscr{C}^0(\overline{\Omega}))^d : \mathbf{v}^h{}_{|K} \in (P_k(K))^d, \forall K \in \mathcal{T}^h, \mathbf{v}^h = \mathbf{0} \text{ on } \Gamma_D \right\}.$$

However, our results would be similar for any $\mathscr{C}^0$-conforming finite element method.

We consider in what follows γ_h, a positive piecewise constant function on the contact interface Γ_C which satisfies for every K that has a non-empty intersection of dimension $d-1$ with Γ_C

$$\gamma_h|_{K \cap \Gamma_C} = \frac{\gamma_0}{h_K}, \tag{5}$$

where γ_0 is a positive given constant (the Nitsche parameter). Note that the value of γ_h on element intersections has no influence.

We next define convenient mesh–dependent norms, in fact weighted $L^2(\Gamma_C)$-norm (since $(\gamma_0/\gamma_h)|_K = h_K$).

Definition 2.1. *For any $v \in L^2(\Gamma_C)$, we set*

$$\|v\|_{-\frac{1}{2},h,\Gamma_C} := \| (\gamma_0/\gamma_h)^{\frac{1}{2}} v\|_{0,\Gamma_C}, \qquad \|v\|_{\frac{1}{2},h,\Gamma_C} := \| (\gamma_h/\gamma_0)^{\frac{1}{2}} v\|_{0,\Gamma_C}.$$

Additionally, it will be convenient to endow $\mathbf{V}^h$ with the following mesh– and parameter–dependent scalar product:

Definition 2.2. *For all $\mathbf{v}^h, \mathbf{w}^h \in \mathbf{V}^h$ we set*

$$(\mathbf{v}^h, \mathbf{w}^h)_{\gamma_h} := (\mathbf{v}^h, \mathbf{w}^h)_{1,\Omega} + (\gamma_h{}^{\frac{1}{2}} v_n^h, \gamma_h{}^{\frac{1}{2}} w_n^h)_{0,\Gamma_C},$$

and note $\|\cdot\|_{\gamma_h} := (\cdot,\cdot)_{\gamma_h}^{\frac{1}{2}}$ the corresponding norm. Remark that the two norms $\|\cdot\|_{\gamma_h}$ and $\|\cdot\|_{1,\Omega}$ are equivalent on $\mathbf{V}^h$, in the following sense (for a quasi-uniform mesh $\mathcal{T}^h$):

$$\|\mathbf{v}^h\|_{1,\Omega} \leq \|\mathbf{v}^h\|_{\gamma_h} \leq \left(1 + C\frac{\gamma_0}{h}\right)^{\frac{1}{2}} \|\mathbf{v}^h\|_{1,\Omega},$$

for any $\mathbf{v}^h \in \mathbf{V}^h$. The positive constant C comes from the trace inequality and the constant of quasi-uniformity of the mesh $\mathcal{T}^h$. For a mesh $\mathcal{T}^h$ that is not quasi-uniform, the same relationship holds, replacing h by $(\min_{K\in\mathcal{T}^h} h_K)$.

We end this section with the following statement: a discrete trace inequality (see, e.g., [53]), that is a key ingredient for the whole mathematical analysis of Nitsche's based methods.

Lemma 2.3. *There exists $C > 0$, independent of the parameter γ_0 and of the mesh size h, such that, for all $\mathbf{v}^h \in \mathbf{V}^h$*

$$\|\sigma_n(\mathbf{v}^h)\|_{-\frac{1}{2},h,\Gamma_C} \leq C\|\mathbf{v}^h\|_{1,\Omega}. \tag{6}$$

2.2 Semi-discrete problem in space

Our Nitsche–based discretization of contact condition is based on the following result (see [3] and as well [9] for a detailed formal proof).

Proposition 2.4. *Let γ be a positive function defined on Γ_C. The contact condition (2) can be reformulated as follows:*

$$\sigma_n(\mathbf{u}) = [\sigma_n(\mathbf{u}) - \gamma\, u_n]_{\mathbb{R}^-}. \tag{7}$$

As in [11, 12] we will consider a family of methods indexed by a parameter $\Theta \in \mathbb{R}$ (with, in general, $\Theta = -1, 0, 1$, see, e.g., [13]). Let us introduce the discrete linear operator

$$\mathrm{P}^{\mathbf{n}}_{\Theta,\gamma_h} : \begin{array}{ccc} \mathbf{V}^h & \to & L^2(\Gamma_C) \\ \mathbf{v}^h & \mapsto & \Theta\sigma_n(\mathbf{v}^h) - \gamma_h v_n^h \end{array}.$$

Define as well the bilinear form:

$$A^{\mathbf{n}}_{\Theta\gamma_h}(\mathbf{u}^h, \mathbf{v}^h) := a(\mathbf{u}^h, \mathbf{v}^h) - \int_{\Gamma_C} \frac{\Theta}{\gamma_h}\, \sigma_n(\mathbf{u}^h)\sigma_n(\mathbf{v}^h)\, d\Gamma.$$

The space semi–discretized Nitsche-based method for unilateral contact problems in elastodynamics then reads (see, e.g, [8, 11]):

$$\begin{cases} \text{Find } \mathbf{u}^h : [0,T] \to \mathbf{V}^h \text{ such that for } t \in [0,T] : \\ (\rho\ddot{\mathbf{u}}^h(t), \mathbf{v}^h)_{0,\Omega} + A^{\mathbf{n}}_{\Theta\gamma_h}(\mathbf{u}^h(t), \mathbf{v}^h) + \displaystyle\int_{\Gamma_C} \frac{1}{\gamma_h}\, [\mathrm{P}^{\mathbf{n}}_{1,\gamma_h}(\mathbf{u}^h(t))]_{\mathbb{R}^-}\, \mathrm{P}^{\mathbf{n}}_{\Theta,\gamma_h}(\mathbf{v}^h)\, d\Gamma \\ \quad = L(t)(\mathbf{v}^h), \qquad \forall\, \mathbf{v}^h \in \mathbf{V}^h, \\ \mathbf{u}^h(0,\cdot) = \mathbf{u}_0^h, \qquad \dot{\mathbf{u}}^h(0,\cdot) = \dot{\mathbf{u}}_0^h, \end{cases} \tag{8}$$

where $\mathbf{u}_0^h$ (resp. $\dot{\mathbf{u}}_0^h$) is an approximation in $\mathbf{V}^h$ of the initial displacement $\mathbf{u}_0$ (resp. the initial velocity $\dot{\mathbf{u}}_0$), for instance the Lagrange interpolant or the $L^2(\Omega)$ projection of $\mathbf{u}_0$ (resp. $\dot{\mathbf{u}}_0$).

Remark 2.5. *Note that, as in [8], we adopted in this presentation a different convention for notations compared to previous works [11, 12]. This is in order to get closer to the formulations provided in most of the papers on Nitsche's method and on the augmented Lagrangian method.*

We can reformulate (8) as a system of (non-linear) second-order differential equations. To this purpose, using Riesz's representation theorem in $(\mathbf{V}^h, (\cdot,\cdot)_{\gamma_h})$ we first introduce the mass operator $\mathbf{M}^h : \mathbf{V}^h \to \mathbf{V}^h$, which is defined for all $\mathbf{v}^h, \mathbf{w}^h \in \mathbf{V}^h$ by $(\mathbf{M}^h\mathbf{v}^h, \mathbf{w}^h)_{\gamma_h} = (\rho\mathbf{v}^h, \mathbf{w}^h)_{0,\Omega}$. Still using Riesz's representation theorem, we define the (non-linear) operator $\mathbf{B}^h : \mathbf{V}^h \to \mathbf{V}^h$, by means of the formula

$$(\mathbf{B}^h\mathbf{v}^h, \mathbf{w}^h)_{\gamma_h} := A^{\mathbf{n}}_{\Theta\gamma_h}(\mathbf{v}^h, \mathbf{w}^h) + \int_{\Gamma_C} \frac{1}{\gamma_h} \left[\mathrm{P}^{\mathbf{n}}_{1,\gamma_h}(\mathbf{v}^h)\right]_{\mathbb{R}^-} \mathrm{P}^{\mathbf{n}}_{\Theta,\gamma_h}(\mathbf{w}^h)\, d\Gamma,$$

for all $\mathbf{v}^h, \mathbf{w}^h \in \mathbf{V}^h$. Finally, we denote by $\mathbf{L}^h(t)$ the vector in $\mathbf{V}^h$ such that, for all $t \in [0,T]$ and for every $\mathbf{w}^h$ in $\mathbf{V}^h$: $(\mathbf{L}^h(t), \mathbf{w}^h)_{\gamma_h} = L(t)(\mathbf{w}^h)$. With the above notation, Problem (8) reads:

$$\begin{cases} \text{Find } \mathbf{u}^h : [0,T] \to \mathbf{V}^h \text{ such that for } t \in [0,T] : \\ \mathbf{M}^h\ddot{\mathbf{u}}^h(t) + \mathbf{B}^h\mathbf{u}^h(t) = \mathbf{L}^h(t), \\ \mathbf{u}^h(0,\cdot) = \mathbf{u}_0^h, \qquad \dot{\mathbf{u}}^h(0,\cdot) = \dot{\mathbf{u}}_0^h. \end{cases} \tag{9}$$

Moreover, we recall the results of well-posedness and the energy estimate for the semi-discrete problem in space, that were established in [11]. First, the following theorem together with the boundedness of $\|(\mathbf{M}^h)^{-1}\|_{\gamma_h}$ (see [11]) show that Problem (8) (or equivalently Problem (9)) is well-posed.

Theorem 2.6. *The operator $\mathbf{B}^h$ is Lipschitz-continuous in the following sense: there exists a constant $C > 0$, independent of h, Θ and γ_0 such that, for all $\mathbf{v}_1^h, \mathbf{v}_2^h \in \mathbf{V}^h$:*

$$\|\mathbf{B}^h\mathbf{v}_1^h - \mathbf{B}^h\mathbf{v}_2^h\|_{\gamma_h} \leq C(1+\gamma_0^{-1})(1+|\Theta|)\|\mathbf{v}_1^h - \mathbf{v}_2^h\|_{\gamma_h}. \tag{10}$$

As a consequence, for every value of $\Theta \in \mathbb{R}$ and $\gamma_0 > 0$, Problem (8) admits one unique solution $\mathbf{u}^h \in \mathscr{C}^2([0,T], \mathbf{V}^h)$.

Remark 2.7. *Note that, conversely to the static case (see [9, 13, 7]) and the fully-discrete case there is no condition on γ_0 for the space (semi-)discretization, which remains well-posed even if γ_0 is arbitrarily small. However, this does not imply that the solution remains consistent when γ_0 becomes small (see Remark 3.6 and Fig. 4 in the sequel).*

We recall that the standard (mixed) finite element semi-discretization for elastodynamics with unilateral contact leads to ill-posed problems (see, e.g., [30, 22]), which is not the case of Nitsche's formulation that leads to a well-posed (Lipschitz) system of differential equations. This feature is shared with the standard penalty method, the difference being that Nitsche's method remains consistent in a strong sense (see [11]). Note that the standard (mixed) finite element semi-discretization is consistent as well as the singular dynamic method introduced in [45]. The mass redistribution method introduced in [30] is asymptotically consistent when h vanishes.

Now we consider the energy estimates which are counterparts of the equation (3), in the semi–discretized case. Let us define the discrete energy as follows:

$$E^h(t) := \frac{1}{2}\rho\|\dot{\mathbf{u}}^h(t)\|^2_{0,\Omega} + \frac{1}{2}a(\mathbf{u}^h(t), \mathbf{u}^h(t)), \quad \forall t \in [0,T].$$

which is associated to the solution $\mathbf{u}^h(t)$ to Problem (8). This is the direct transposition of the mechanical energy $E(t)$ from the continuous system. As in [11], we define also a modified energy more suited to Nitsche's method

$$E^h_\Theta(t) := E^h(t) - \frac{\Theta}{2\gamma_0}\left[\left\|\sigma_n(\mathbf{u}^h(t))\right\|^2_{-\frac{1}{2},h,\Gamma_C} - \left\|\left[\mathrm{P}^{\mathbf{n}}_{1,\gamma_h}(\mathbf{u}^h(t))\right]_{\mathbb{R}^-}\right\|^2_{-\frac{1}{2},h,\Gamma_C}\right] := E^h(t) - \Theta R^h(t), \quad (11)$$

in which a consistent term is added. This term denoted $R^h(t)$ represents, roughly speaking, the non-fulfillment of the contact condition (7) by $\mathbf{u}^h$. The relationship between $E^h(t)$ and $E^h_\Theta(t)$ is provided in the Lemma below:

Proposition 2.8. *For $\Theta \geq 0$ and γ_0 large enough, there exists $C > 0$ independent of h, of γ_0 and of the solution to Problem (8), such that, for all $t \in [0,T]$:*

$$E^h(t) \leq C E^h_\Theta(t).$$

Proof. This result is obtained using the coercivity of $a(\cdot,\cdot)$ and applying Lemma 2.3. □

Remark 2.9. *For $\Theta < 0$, such a result with a constant independent of the mesh parameter h cannot be obtained. As a consequence, for $\Theta < 0$, the quantity $E^h_\Theta(t)$ cannot be used for optimal energy evolution estimates and might become even negative for h small.*

Still in [11], the following evolution of E^h_Θ is obtained:

Theorem 2.10. *Suppose that the system associated to (1)–(2) is conservative, i.e., that $L(t) \equiv 0$ for all $t \in [0,T]$. The solution $\mathbf{u}^h$ to (8) then satisfies the following identity:*

$$\frac{d}{dt}E^h_\Theta(t) = (1-\Theta)\int_{\Gamma_C}\left[\mathrm{P}^{\mathbf{n}}_{1,\gamma_h}(\mathbf{u}^h(t))\right]_{\mathbb{R}^-}\dot{u}^h_n(t)\,d\Gamma.$$

Notably, when $\Theta = 1$, we get for any $t \in [0,T]$: $E^h_1(t) = E^h_1(0)$.

This result links the non-satisfaction of the energy conservation to the non-satisfaction of the so-called persistency condition. However, it appears in the present study that it would be preferable to use $E^h_1(t)$ even for the variants $\Theta \neq 1$ (see Remark 2.9 and Section 3), for which the following result can be established:

Theorem 2.11. *Suppose that the system associated to (1)–(2) is conservative, i.e., that $L(t) \equiv 0$ for all $t \in [0,T]$. The solution $\mathbf{u}^h$ to (8) then satisfies the following identity:*

$$\frac{d}{dt}E^h_1(t) = (1-\Theta)\int_{\Gamma_C}\frac{1}{\gamma_h}\left(\left[\mathrm{P}^{\mathbf{n}}_{1,\gamma_h}(\mathbf{u}^h(t))\right]_{\mathbb{R}^-} - \sigma_n(\mathbf{u}^h(t))\right)\,\sigma_n(\dot{\mathbf{u}}^h(t))\,d\Gamma.$$

Proof. Let us take $\mathbf{v}^h = \dot{\mathbf{u}}^h(t)$ in (8):

$$(\rho\ddot{\mathbf{u}}^h(t), \dot{\mathbf{u}}^h(t))_{0,\Omega} + A^{\mathbf{n}}_{\Theta\gamma_h}(\mathbf{u}^h(t), \dot{\mathbf{u}}^h(t)) + \int_{\Gamma_C}\frac{1}{\gamma_h}\left[\mathrm{P}^{\mathbf{n}}_{1,\gamma_h}(\mathbf{u}^h(t))\right]_{\mathbb{R}^-}\mathrm{P}^{\mathbf{n}}_{\Theta,\gamma_h}(\dot{\mathbf{u}}^h(t))\,d\Gamma = 0,$$

which we reformulate as:

$$\frac{d}{dt}E^h(t) - \Theta\int_{\Gamma_C}\frac{1}{\gamma_h}\sigma_n(\mathbf{u}^h(t))\sigma_n(\dot{\mathbf{u}}^h(t))\,d\Gamma + \int_{\Gamma_C}\frac{1}{\gamma_h}\left[\mathrm{P}^{\mathbf{n}}_{1,\gamma_h}(\mathbf{u}^h(t))\right]_{\mathbb{R}^-}\mathrm{P}^{\mathbf{n}}_{\Theta,\gamma_h}(\dot{\mathbf{u}}^h(t))\,d\Gamma = 0.$$

We split the second term, use $\mathrm{P}^{\mathbf{n}}_{\Theta,\gamma_h}(\dot{\mathbf{u}}^h(t)) = \Theta\sigma_n(\dot{\mathbf{u}}^h(t)) - \gamma_h \dot{u}^h_n = \mathrm{P}^{\mathbf{n}}_{1,\gamma_h}(\dot{\mathbf{u}}^h(t)) + (\Theta-1)\,\sigma_n(\dot{\mathbf{u}}^h(t))$ and get:

$$\frac{d}{dt}E^h(t) - \int_{\Gamma_C}\frac{1}{\gamma_h}\sigma_n(\mathbf{u}^h(t))\sigma_n(\dot{\mathbf{u}}^h(t))\,d\Gamma - (\Theta-1)\int_{\Gamma_C}\frac{1}{\gamma_h}\sigma_n(\mathbf{u}^h(t))\sigma_n(\dot{\mathbf{u}}^h(t))\,d\Gamma$$
$$+\int_{\Gamma_C}\frac{1}{\gamma_h}\left[\mathrm{P}^{\mathbf{n}}_{1,\gamma_h}(\mathbf{u}^h(t))\right]_{\mathbb{R}^-}\left(\mathrm{P}^{\mathbf{n}}_{1,\gamma_h}(\dot{\mathbf{u}}^h(t)) + (\Theta-1)\sigma_n(\dot{\mathbf{u}}^h(t))\right)\,d\Gamma = 0.$$

The result is obtained by re-ordering the terms, using the property $\frac{d}{dt}\frac{1}{2}[x(t)]^2_{\mathbb{R}^-} = [x(t)]_{\mathbb{R}^-}\dot{x}(t)$ and the definition of $E^h_1(t)$. □

Remark 2.12. *The above result still states that $E^h_1(t)$ is conserved for the symmetric variant $\Theta = 1$, and, for $\Theta \neq 1$ the variations of $E^h_1(t)$ comes from the non-fulfillment of the contact condition (7) by $\mathbf{u}^h$.*

2.3 Verlet scheme

Let $\tau > 0$ be the time–step, and consider a uniform discretization of the time interval $[0,T]$: $(t^0,\ldots,t^N)$, with $t^n = n\tau$, $n = 0,\ldots,N$. Let $\theta \in [0,1]$, we use the notation:

$$\mathbf{x}^{h,n+\theta} = (1-\theta)\mathbf{x}^{h,n} + \theta\mathbf{x}^{h,n+1}$$

for arbitrary quantities $\mathbf{x}^{h,n}, \mathbf{x}^{h,n+1} \in \mathbf{V}^h$. Hereafter we denote by $\mathbf{u}^{h,n}$ (resp. $\dot{\mathbf{u}}^{h,n}$ and $\ddot{\mathbf{u}}^{h,n}$) the resulting discretized displacement (resp. velocity and acceleration) at time-step t^n.

The discretization of Problem (9) with the velocity-Verlet scheme reads:

$$\begin{cases} \text{Find } \mathbf{u}^{h,n+1}, \dot{\mathbf{u}}^{h,n+1}, \ddot{\mathbf{u}}^{h,n+1} \in \mathbf{V}^h \text{ such that:} \\ \mathbf{u}^{h,n+1} = \mathbf{u}^{h,n} + \tau\dot{\mathbf{u}}^{h,n} + \dfrac{\tau^2}{2}\ddot{\mathbf{u}}^{h,n}, \\ \dot{\mathbf{u}}^{h,n+1} = \dot{\mathbf{u}}^{h,n} + \tau\ddot{\mathbf{u}}^{h,n+\frac{1}{2}}, \\ \mathbf{M}^h\ddot{\mathbf{u}}^{h,n+1} + \mathbf{B}^h\mathbf{u}^{h,n+1} = \mathbf{L}^{h,n+1}, \end{cases} \tag{12}$$

with initial conditions $\mathbf{u}^{h,0} = \mathbf{u}^h_0$, $\dot{\mathbf{u}}^{h,0} = \dot{\mathbf{u}}^h_0$ and $\ddot{\mathbf{u}}^{h,0} = \ddot{\mathbf{u}}^h_0$, and the notation $\mathbf{L}^{h,n+1} = \mathbf{L}^h(t^{n+1})$, the initial value $\ddot{\mathbf{u}}^h_0$ being obtained through $\mathbf{M}^h\ddot{\mathbf{u}}^h_0 = \mathbf{L}^{h,0} - \mathbf{B}^h\mathbf{u}^{h,0}$.

This scheme corresponds to the variant of the Newmark scheme with $\gamma = \frac{1}{2}$ and $\beta = 0$ (see, e.g., [11, 22]). As a result, this is a second order consistent scheme in τ. Note that, for practical implementation, the acceleration can be eliminated using the relationship $\mathbf{M}^h\ddot{\mathbf{u}}^{h,n} = \mathbf{L}^{h,n} - \mathbf{B}^h\mathbf{u}^{h,n}$. This result into the following reformulation, where the only unknowns are the displacement and the velocity:

$$\begin{cases} \text{Find } \mathbf{u}^{h,n+1}, \dot{\mathbf{u}}^{h,n+1} \in \mathbf{V}^h \text{ such that:} \\ \mathbf{M}^h\mathbf{u}^{h,n+1} = \mathbf{M}^h\mathbf{u}^{h,n} + \tau\mathbf{M}^h\dot{\mathbf{u}}^{h,n} + \dfrac{\tau^2}{2}\left(\mathbf{L}^{h,n} - \mathbf{B}^h\mathbf{u}^{h,n}\right), \\ \dot{\mathbf{u}}^{h,n+1} = \dot{\mathbf{u}}^{h,n} + \tau\left(\mathbf{L}^{h,n+\frac{1}{2}} - (\mathbf{B}^h\mathbf{u}^h)^{n+\frac{1}{2}}\right). \end{cases} \tag{13}$$

Since this scheme only requires the inversion of the mass matrix $\mathbf{M}^h$ at each time–step, it becomes then fully explicit when the mass matrix $\mathbf{M}^h$ is lumped.

We can transform the scheme (12) into a two–steps scheme. Indeed, the first equation of (12) applied for time-steps n and $n+1$ reads:

$$\frac{\tau^2}{2}\ddot{\mathbf{u}}^{h,n-1} = \mathbf{u}^{h,n} - \mathbf{u}^{h,n-1} - \tau\dot{\mathbf{u}}^{h,n-1}, \quad \frac{\tau^2}{2}\ddot{\mathbf{u}}^{h,n} = \mathbf{u}^{h,n+1} - \mathbf{u}^{h,n} - \tau\dot{\mathbf{u}}^{h,n}. \tag{14}$$

So, using the above relationships, the second equation of (12), at time-step n, can be written as

$$\tau\dot{\mathbf{u}}^{h,n} = \tau\dot{\mathbf{u}}^{h,n-1} + \frac{\tau^2}{2}(\ddot{\mathbf{u}}^{h,n} + \ddot{\mathbf{u}}^{h,n-1}) = \tau\dot{\mathbf{u}}^{h,n-1} + \frac{\tau^2}{2}\ddot{\mathbf{u}}^{h,n} + \left(\mathbf{u}^{h,n} - \mathbf{u}^{h,n-1} - \tau\dot{\mathbf{u}}^{h,n-1}\right)$$

which can be simplified as:

$$\tau\dot{\mathbf{u}}^{h,n} = \frac{\tau^2}{2}\ddot{\mathbf{u}}^{h,n} + (\mathbf{u}^{h,n} - \mathbf{u}^{h,n-1}).$$

We add the above equation to the second relationship in (14) and get

$$\tau^2\ddot{\mathbf{u}}^{h,n} = \mathbf{u}^{h,n+1} - 2\mathbf{u}^{h,n} + \mathbf{u}^{h,n-1}.$$

Using finally the third equation in (12), combined with the above relationship, we obtain:

$$\begin{cases} \text{Find } \mathbf{u}^{h,n+1} \in \mathbf{V}^h \text{ such that:} \\ \mathbf{M}^h \dfrac{\mathbf{u}^{h,n+1} - 2\mathbf{u}^{h,n} + \mathbf{u}^{h,n-1}}{\tau^2} + \mathbf{B}^h\mathbf{u}^{h,n} = \mathbf{L}^{h,n}. \end{cases} \tag{15}$$

This is a two–steps scheme, so called Störmer-Verlet scheme or central difference scheme, that involves only the displacement as an unknown (the first step $\mathbf{u}^{h,1}$ is classically obtained via the first equation of (13) at $n = 0$). Note finally that Leapfrog scheme is also equivalent to Verlet one (see e.g. [16, 27]): it suffices to define an intermediate velocity $\dot{\mathbf{u}}^{h,[n+\frac{1}{2}]}$ at half–time–steps $t^{n+\frac{1}{2}}$ as follows:

$$\dot{\mathbf{u}}^{h,[n+\frac{1}{2}]} = \dot{\mathbf{u}}^{h,n} + \frac{\tau}{2}\ddot{\mathbf{u}}^{h,n},$$

where we used the notation $\dot{\mathbf{u}}^{h,[n+\frac{1}{2}]}$ so as to differentiate this new unknown from $\dot{\mathbf{u}}^{h,n+\frac{1}{2}}$ defined earlier. Using this new intermediate velocity, the scheme (12) is reformulated as:

$$\begin{cases} \text{Find } \mathbf{u}^{h,n+1}, \dot{\mathbf{u}}^{h,[n+\frac{1}{2}]}, \ddot{\mathbf{u}}^{h,n+1} \in \mathbf{V}^h \text{ such that:} \\ \dot{\mathbf{u}}^{h,[n+\frac{1}{2}]} = \dot{\mathbf{u}}^{h,[n-\frac{1}{2}]} + \tau\ddot{\mathbf{u}}^{h,n}, \\ \mathbf{u}^{h,n+1} = \mathbf{u}^{h,n} + \tau\dot{\mathbf{u}}^{h,[n+\frac{1}{2}]}, \\ \mathbf{M}^h\ddot{\mathbf{u}}^{h,n+1} + \mathbf{B}^h\mathbf{u}^{h,n+1} = \mathbf{L}^{h,n+1}, \end{cases} \tag{16}$$

with initial conditions $\mathbf{u}^{h,0} = \mathbf{u}_0^h$, $\dot{\mathbf{u}}^{h,[1/2]} = \dot{\mathbf{u}}_0^h + \frac{\tau}{2}\ddot{\mathbf{u}}_0^h$.

3 Stability properties of Verlet scheme

First, in 3.1, we present different energies associated to the solution to Problem (12), and make explicit their relationships. Then, in 3.2, we derive energy estimates associated to the fully discrete Problem (12), and a (non-optimal) stability result is deduced in 3.3. We conclude in 3.4 with some comments and arguments that a better result may be expected.

3.1 Discrete energies

We next define the following energy:

$$E^{h,n} := \frac{1}{2}\rho\|\dot{\mathbf{u}}^{h,n}\|_{0,\Omega}^2 + \frac{1}{2}a(\mathbf{u}^{h,n},\mathbf{u}^{h,n}),$$

which is associated with the solution $\mathbf{u}^{h,n}$ to Problem (12). Set also

$$E_\Theta^{h,n} := E^{h,n} - \frac{\Theta}{2\gamma_0}\left[\left\|\sigma_n(\mathbf{u}^{h,n})\right\|^2_{-\frac{1}{2},h,\Gamma_C} - \left\|[\mathrm{P}^{\mathbf{n}}_{1,\gamma_h}(\mathbf{u}^{h,n})]_{\mathbb{R}^-}\right\|^2_{-\frac{1}{2},h,\Gamma_C}\right] := E^{h,n} - \Theta R^{h,n}.$$

Note that the energies $E^{h,n}$ and $E_\Theta^{h,n}$ are the fully discrete counterparts of the semi–discrete energies $E^h(t)$ and $E_\Theta^h(t)$. Note additionnally that a result similar to Proposition 2.8 can be established, that allows to bound the physical energy by the augmented energy under appropriate conditions on the numerical parameters (and the statement of Remark 2.9 still applies):

Proposition 3.1. *For $\Theta \geq 0$ and γ_0 large enough, there exists $C > 0$ independent of h, of γ_0 and of the solution to Problem (12), such that, for all $n = 0, \ldots, N$:*

$$E^{h,n} \leq C E_\Theta^{h,n}.$$

To simplify slightly the notations in the energy estimates below, we will make use of the convention: $\mathrm{P}^n := \mathrm{P}^{\mathbf{n}}_{1,\gamma_h}(\mathbf{u}^{h,n})$ for any $n \in \mathbb{N}$. We will denote as well by $[\cdot]_{\mathbb{R}^+}$ the projection onto $\mathbb{R}^+$. Additionally, we define a modified energy adapted to the Verlet scheme:

$$E^{h,\tau,n} := E_1^{h,n} - \frac{\rho\tau^2}{8}\|\ddot{\mathbf{u}}^{h,n}\|_{0,\Omega}^2.$$

Of course, this variant of the energy definition makes also sense and is usable for stability analysis only if it can be used to bound the physical energy $E^{h,n}$. This is the aim of the following result:

Proposition 3.2. *Suppose that $L^n \equiv 0$ for all $n = 0, \ldots, N$ and that the mesh $\mathcal{T}^h$ is quasi-uniform. Then, for γ_0 large enough and $\frac{\tau}{h}$ small enough, there exists $C > 0$, independent of h, of γ_0 and of the solution to Problem (12), such that, for all $n = 0, \ldots, N$:*

$$E^{h,n} \leq C E^{h,\tau,n}.$$

Proof. We suppose $L^n \equiv 0$ and take $\mathbf{v}^h = \ddot{\mathbf{u}}^{h,n}$ in Problem (12):

$$\rho\|\ddot{\mathbf{u}}^{h,n}\|_{0,\Omega}^2 = -A^{\mathbf{n}}_{\Theta\gamma_h}(\mathbf{u}^{h,n},\ddot{\mathbf{u}}^{h,n}) - \int_{\Gamma_C}\frac{1}{\gamma_h}\,[\mathrm{P}^{\mathbf{n}}_{1,\gamma_h}(\mathbf{u}^{h,n})]_{\mathbb{R}^-}\,\mathrm{P}^{\mathbf{n}}_{\Theta,\gamma_h}(\ddot{\mathbf{u}}^{h,n})\,d\Gamma. \tag{17}$$

We assume that γ_0 is large enough, then use the Cauchy-Schwarz inequality, the Lemma 2.3 and the inverse inequality [25, Corollary 1.141, Remark 1.143] to bound the first right term:

$$|A^{\mathbf{n}}_{\Theta\gamma_h}(\mathbf{u}^{h,n},\ddot{\mathbf{u}}^{h,n})| \leq C\|\mathbf{u}^{h,n}\|_{1,\Omega}\|\ddot{\mathbf{u}}^{h,n}\|_{1,\Omega} \leq \frac{C}{h}\|\mathbf{u}^{h,n}\|_{1,\Omega}\|\ddot{\mathbf{u}}^{h,n}\|_{0,\Omega},$$

with $C > 0$ independent of γ_0 and h. We use the Cauchy-Schwarz inequality for the second term:

$$\begin{aligned}&\left|\int_{\Gamma_C}\frac{1}{\gamma_h}\,[\mathrm{P}^{\mathbf{n}}_{1,\gamma_h}(\mathbf{u}^{h,n})]_{\mathbb{R}^-}\,\mathrm{P}^{\mathbf{n}}_{\Theta,\gamma_h}(\ddot{\mathbf{u}}^{h,n})\,d\Gamma\right| \\ &\leq \left(\int_{\Gamma_C}\frac{1}{\gamma_h}\,[\mathrm{P}^{\mathbf{n}}_{1,\gamma_h}(\mathbf{u}^{h,n})]^2_{\mathbb{R}^-}\,d\Gamma\right)^{1/2}\left(\int_{\Gamma_C}\frac{1}{\gamma_h}\,(\mathrm{P}^{\mathbf{n}}_{\Theta,\gamma_h}(\ddot{\mathbf{u}}^{h,n}))^2\,d\Gamma\right)^{1/2}.\end{aligned}$$

Using once more Lemma 2.3 we bound:

$$\int_{\Gamma_C} \frac{1}{\gamma_h} (\mathrm{P}^{\mathbf{n}}_{\Theta,\gamma_h}(\ddot{\mathbf{u}}^{h,n}))^2 \, d\Gamma \leq 2 \int_{\Gamma_C} \left(\frac{\Theta^2}{\gamma_h} {\sigma_n}^2(\ddot{\mathbf{u}}^{h,n}) + \gamma_h (\ddot{u}_n^{h,n})^2 \right) d\Gamma \leq C \|\ddot{\mathbf{u}}^{h,n}\|^2_{1,\Omega} + 2\gamma_0 \|\ddot{u}_n^{h,n}\|^2_{\frac{1}{2},h,\Gamma_C},$$

still with $C > 0$ independent of h and γ_0. We then use the trace inequality [6, Theorem 1.6.6] and the inverse inequality [25, Corollary 1.141, Remark 1.143] and get:

$$\|\ddot{u}_n^{h,n}\|^2_{\frac{1}{2},h,\Gamma_C} \leq \frac{C}{h} \|\ddot{u}_n^{h,n}\|^2_{0,\Gamma_C} \leq \frac{C}{h} \|\ddot{\mathbf{u}}^{h,n}\|_{0,\Omega} \|\ddot{\mathbf{u}}^{h,n}\|_{1,\Omega} \leq \frac{C}{h^2} \|\ddot{\mathbf{u}}^{h,n}\|^2_{0,\Omega}.$$

We insert the above bounds into (17), take into account that γ_0 is large, apply once again the inverse inequality and get:

$$\begin{aligned}
& \rho \|\ddot{\mathbf{u}}^{h,n}\|^2_{0,\Omega} \\
\leq \; & \frac{C}{h} \|\mathbf{u}^{h,n}\|_{1,\Omega} \|\ddot{\mathbf{u}}^{h,n}\|_{0,\Omega} + C \gamma_0^{-\frac{1}{2}} \|[\mathrm{P}^{\mathbf{n}}_{1,\gamma_h}(\mathbf{u}^{h,n})]_{\mathbb{R}^-}\|_{-\frac{1}{2},h,\Gamma_C} \left(\|\ddot{\mathbf{u}}^{h,n}\|^2_{1,\Omega} + \frac{\gamma_0}{h^2} \|\ddot{\mathbf{u}}^{h,n}\|^2_{0,\Omega} \right)^{\frac{1}{2}} \\
\leq \; & \frac{C}{h} \|\mathbf{u}^{h,n}\|_{1,\Omega} \|\ddot{\mathbf{u}}^{h,n}\|_{0,\Omega} + C \frac{\gamma_0^{-\frac{1}{2}} (1+\gamma_0)^{\frac{1}{2}}}{h} \|[\mathrm{P}^{\mathbf{n}}_{1,\gamma_h}(\mathbf{u}^{h,n})]_{\mathbb{R}^-}\|_{-\frac{1}{2},h,\Gamma_C} \|\ddot{\mathbf{u}}^{h,n}\|_{0,\Omega} \\
\leq \; & \frac{C}{h} \left(\|\mathbf{u}^{h,n}\|_{1,\Omega} + \|[\mathrm{P}^{\mathbf{n}}_{1,\gamma_h}(\mathbf{u}^{h,n})]_{\mathbb{R}^-}\|_{-\frac{1}{2},h,\Gamma_C} \right) \|\ddot{\mathbf{u}}^{h,n}\|_{0,\Omega}.
\end{aligned}$$

As a result, we obtain

$$\rho \|\ddot{\mathbf{u}}^{h,n}\|_{0,\Omega} \leq \frac{C}{h} (\|\mathbf{u}^{h,n}\|_{1,\Omega} + \|[\mathrm{P}^{\mathbf{n}}_{1,\gamma_h}(\mathbf{u}^{h,n})]_{\mathbb{R}^-}\|_{-\frac{1}{2},h,\Gamma_C}), \tag{18}$$

which allows to conclude that $E_1^{h,n} \leq C E^{h,\tau,n}$ for $\frac{\tau}{h}$ small enough using the coercivity of $a(\cdot,\cdot)$. The estimate $E^{h,n} \leq C E^{h,\tau,n}$ is then deduced from Proposition 3.1. □

3.2 Energy evolution estimates

First, the straightforward adaptation of [12, Proposition 3.4], taking $\gamma = \frac{1}{2}$ and $\beta = 0$ for Verlet scheme gives the following energy identity:

Proposition 3.3. *Suppose that $L^n \equiv 0$ for all $n \geq 0$. The following energy identity holds for all $n \geq 0$:*

$$\begin{aligned}
E_\Theta^{h,n+1} - E_\Theta^{h,n} = \; & \Theta \int_{\Gamma_C} \frac{1}{2\gamma_h} \left(\left[\mathrm{P}^{n+1}\right]_{\mathbb{R}^-} [\mathrm{P}^n]_{\mathbb{R}^+} - [\mathrm{P}^n]_{\mathbb{R}^-} \left[\mathrm{P}^{n+1}\right]_{\mathbb{R}^+} \right) d\Gamma \\
& - \frac{\tau}{4} \left[A^{\mathbf{n}}_{\Theta\gamma_h}(\mathbf{u}^{h,n+1} - \mathbf{u}^{h,n}, \dot{\mathbf{u}}^{h,n+1} - \dot{\mathbf{u}}^{h,n}) \right. \\
& \left. + \int_{\Gamma_C} \frac{1}{\gamma_h} \left(\left[\mathrm{P}^{n+1}\right]_{\mathbb{R}^-} - [\mathrm{P}^n]_{\mathbb{R}^-} \right) \mathrm{P}^{\mathbf{n}}_{\Theta,\gamma_h}(\dot{\mathbf{u}}^{h,n+1} - \dot{\mathbf{u}}^{h,n}) \, d\Gamma \right] \\
& + (1-\Theta) \int_{\Gamma_C} \frac{1}{2} \left(\left[\mathrm{P}^{n+1}\right]_{\mathbb{R}^-} + [\mathrm{P}^n]_{\mathbb{R}^-} \right) \left(u_n^{h,n+1} - u_n^{h,n} \right) d\Gamma.
\end{aligned} \tag{19}$$

This result can be easily adapted to the case where $E_1^{h,n}$ is considered even for $\Theta \neq 1$ as follows:

Proposition 3.4. *Suppose that $L^n \equiv 0$ for all $n \geq 0$. The following energy identity holds for all $n \geq 0$:*

$$
\begin{aligned}
&E_1^{h,n+1} - E_1^{h,n} \\
&= \int_{\Gamma_C} \frac{1}{2\gamma_h} \left(\left[\mathrm{P}^{n+1}\right]_{\mathbb{R}^-} \left[\mathrm{P}^n\right]_{\mathbb{R}^+} - \left[\mathrm{P}^n\right]_{\mathbb{R}^-} \left[\mathrm{P}^{n+1}\right]_{\mathbb{R}^+} \right) d\Gamma \\
&\quad - \frac{\tau}{4} \left[A^{\mathbf{n}}_{\Theta\gamma_h}(\mathbf{u}^{h,n+1} - \mathbf{u}^{h,n}, \dot{\mathbf{u}}^{h,n+1} - \dot{\mathbf{u}}^{h,n}) \right. \\
&\quad \left. + \int_{\Gamma_C} \frac{1}{\gamma_h} \left(\left[\mathrm{P}^{n+1}\right]_{\mathbb{R}^-} - \left[\mathrm{P}^n\right]_{\mathbb{R}^-} \right) \mathrm{P}^{\mathbf{n}}_{\Theta,\gamma_h}(\dot{\mathbf{u}}^{h,n+1} - \dot{\mathbf{u}}^{h,n}) \, d\Gamma \right] \qquad (20) \\
&\quad + (1-\Theta) \int_{\Gamma_C} \frac{1}{2\gamma_h} \left(\left[\mathrm{P}^{n+1}\right]_{\mathbb{R}^-} + \left[\mathrm{P}^n\right]_{\mathbb{R}^-} - \sigma_n(\mathbf{u}^{h,n+1}) - \sigma_n(\mathbf{u}^{h,n}) \right) \sigma_n\left(\mathbf{u}^{h,n+1} - \mathbf{u}^{h,n}\right) d\Gamma.
\end{aligned}
$$

Proof. This identity is deduced from

$$
\begin{aligned}
&E_1^{h,n+1} - E_1^{h,n} \\
&= E_\Theta^{h,n+1} - E_\Theta^{h,n} + (1-\Theta) \int_{\Gamma_C} \frac{1}{2\gamma_h} \left(\left[\mathrm{P}^{n+1}\right]^2_{\mathbb{R}^-} - \left[\mathrm{P}^n\right]^2_{\mathbb{R}^-} - {\sigma_n}^2(\mathbf{u}^{h,n+1}) + {\sigma_n}^2(\mathbf{u}^{h,n}) \right) d\Gamma,
\end{aligned}
$$

combined with the following rearrangement (where we use the identity $\left[\mathrm{P}^n\right]_{\mathbb{R}^-} = \sigma_n(\mathbf{u}^{h,n}) - \gamma_h u_n^{h,n} - \left[\mathrm{P}^n\right]_{\mathbb{R}^+}$):

$$
\begin{aligned}
&\left[\mathrm{P}^{n+1}\right]^2_{\mathbb{R}^-} - \left[\mathrm{P}^n\right]^2_{\mathbb{R}^-} - {\sigma_n}^2(\mathbf{u}^{h,n+1}) + {\sigma_n}^2(\mathbf{u}^{h,n}) \\
&= \left(\left[\mathrm{P}^{n+1}\right]_{\mathbb{R}^-} + \left[\mathrm{P}^n\right]_{\mathbb{R}^-} \right) \left(\left[\mathrm{P}^{n+1}\right]_{\mathbb{R}^-} - \left[\mathrm{P}^n\right]_{\mathbb{R}^-} \right) \\
&\quad - \left(\sigma_n(\mathbf{u}^{h,n+1}) + \sigma_n(\mathbf{u}^{h,n}) \right) \left(\sigma_n(\mathbf{u}^{h,n+1}) - \sigma_n(\mathbf{u}^{h,n}) \right) \\
&= \left(\left[\mathrm{P}^{n+1}\right]_{\mathbb{R}^-} + \left[\mathrm{P}^n\right]_{\mathbb{R}^-} - \sigma_n(\mathbf{u}^{h,n+1}) - \sigma_n(\mathbf{u}^{h,n}) \right) \left(\sigma_n(\mathbf{u}^{h,n+1}) - \sigma_n(\mathbf{u}^{h,n}) \right) \\
&\quad - \left(\left[\mathrm{P}^{n+1}\right]_{\mathbb{R}^-} + \left[\mathrm{P}^n\right]_{\mathbb{R}^-} \right) \left(\left[\mathrm{P}^{n+1}\right]_{\mathbb{R}^+} - \left[\mathrm{P}^n\right]_{\mathbb{R}^+} + \gamma_h u_n^{h,n+1} - \gamma_h u_n^{h,n} \right) \\
&= \left(\left[\mathrm{P}^{n+1}\right]_{\mathbb{R}^-} + \left[\mathrm{P}^n\right]_{\mathbb{R}^-} - \sigma_n(\mathbf{u}^{h,n+1}) - \sigma_n(\mathbf{u}^{h,n}) \right) \left(\sigma_n(\mathbf{u}^{h,n+1}) - \sigma_n(\mathbf{u}^{h,n}) \right) \\
&\quad + \left(\left[\mathrm{P}^{n+1}\right]_{\mathbb{R}^-} \left[\mathrm{P}^n\right]_{\mathbb{R}^+} - \left[\mathrm{P}^n\right]_{\mathbb{R}^-} \left[\mathrm{P}^{n+1}\right]_{\mathbb{R}^+} \right) - \left(\left[\mathrm{P}^{n+1}\right]_{\mathbb{R}^-} + \left[\mathrm{P}^n\right]_{\mathbb{R}^-} \right) \left(\gamma_h u_n^{h,n+1} - \gamma_h u_n^{h,n} \right)
\end{aligned}
$$

and gathering the terms with the ones in the expression (19) of Proposition 3.3. □

As an interesting consequence, we obtain the following result for the discrete energy $E^{h,\tau,n}$ by simplifying the previous one:

Proposition 3.5. *Suppose that $L^n \equiv 0$ for all $n \geq 0$. The following energy identity holds for all $n \geq 0$:*

$$
\begin{aligned}
&E^{h,\tau,n+1} - E^{h,\tau,n} \\
&= \int_{\Gamma_C} \frac{1}{2\gamma_h} \left(\left[\mathrm{P}^{n+1}\right]_{\mathbb{R}^-} \left[\mathrm{P}^n\right]_{\mathbb{R}^+} - \left[\mathrm{P}^n\right]_{\mathbb{R}^-} \left[\mathrm{P}^{n+1}\right]_{\mathbb{R}^+} \right) d\Gamma \qquad (21) \\
&\quad + (1-\Theta) \int_{\Gamma_C} \frac{1}{2\gamma_h} \left(\left[\mathrm{P}^{n+1}\right]_{\mathbb{R}^-} + \left[\mathrm{P}^n\right]_{\mathbb{R}^-} - \sigma_n(\mathbf{u}^{h,n+1}) - \sigma_n(\mathbf{u}^{h,n}) \right) \sigma_n\left(\mathbf{u}^{h,n+1} - \mathbf{u}^{h,n}\right) d\Gamma.
\end{aligned}
$$

Proof. We use equations (12) to rewrite:

$$
\begin{aligned}
-\frac{\tau}{4}\Big[A^{\mathbf{n}}_{\Theta\gamma_h}(\mathbf{u}^{h,n+1}-\mathbf{u}^{h,n},\dot{\mathbf{u}}^{h,n+1}-\dot{\mathbf{u}}^{h,n})+\int_{\Gamma_C}\frac{1}{\gamma_h}\left(\left[\mathrm{P}^{n+1}\right]_{\mathbb{R}^-}-\left[\mathrm{P}^{n}\right]_{\mathbb{R}^-}\right)\mathrm{P}^{\mathbf{n}}_{\Theta,\gamma_h}(\dot{\mathbf{u}}^{h,n+1}-\dot{\mathbf{u}}^{h,n})\,d\Gamma\Big]\\
=\frac{\tau}{4}\int_\Omega\rho(\ddot{\mathbf{u}}^{h,n+1}-\ddot{\mathbf{u}}^{h,n})\cdot(\dot{\mathbf{u}}^{h,n+1}-\dot{\mathbf{u}}^{h,n})\,d\Omega=\frac{\tau^2}{8}\int_\Omega\rho(\ddot{\mathbf{u}}^{h,n+1}-\ddot{\mathbf{u}}^{h,n})\cdot(\ddot{\mathbf{u}}^{h,n+1}+\ddot{\mathbf{u}}^{h,n})\,d\Omega\\
=\frac{\rho\tau^2}{8}\|\ddot{\mathbf{u}}^{h,n+1}\|^2_{0,\Omega}-\frac{\rho\tau^2}{8}\|\ddot{\mathbf{u}}^{h,n}\|^2_{0,\Omega}.
\end{aligned}
$$

Then we just use the above identity in (20). □

Remark 3.6. *For γ_0 small, the property of Proposition 3.2 can be lost and the energy $E_1^{h,n}$ may become negative. In that case, some deformation corresponding to a negative energy may exist, which is of course a non-physical situation. This highlights that, even thought the semi–discrete problem* (9) *has a unique solution for γ_0 small, the reliability of the discretization is guaranteed only for γ_0 large enough.*

Remark 3.7. *Still referring to [12, Proposition 3.4], and instead of Verlet scheme, if we consider the explicit Newmark scheme $\gamma = 1$ and $\beta = 0$ and $\Theta = 1$ as Nitsche's variant, the pending energy evolution corresponding to Proposition 3.5 in that case involves the sole term $\left[\mathrm{P}^{n+1}\right]_{\mathbb{R}^-}\left[\mathrm{P}^{n}\right]_{\mathbb{R}^+}$ (instead of $\left[\mathrm{P}^{n+1}\right]_{\mathbb{R}^-}\left[\mathrm{P}^{n}\right]_{\mathbb{R}^+}-\left[\mathrm{P}^{n}\right]_{\mathbb{R}^-}\left[\mathrm{P}^{n+1}\right]_{\mathbb{R}^+}$ for Verlet scheme). This term being non-positive, the stability of this explicit scheme can be established thanks to Proposition 3.2 for $\frac{\tau}{h}$ small enough.*

3.3 Stability analysis in the case $\Theta = 1$

The main result of this section is the following (non-optimal) stability result for the scheme (12) in the case $\Theta = 1$:

Proposition 3.8. *Suppose that $L^n \equiv 0$ for all $n \geq 0$ and that the mesh $\mathcal{T}^h$ is quasi-uniform. Then, for $\Theta = 1$, for γ_0 large enough and for*

$$\gamma_0\tau \leq Ch^2 \tag{22}$$

with $C > 0$ independent of γ_0, h and τ, the energies $E^{h,\tau,n}$ and $E^{h,n}$ remain bounded.

Proof. We already know from Proposition 3.5 that, for $\Theta = 1$:

$$E^{h,\tau,n+1}-E^{h,\tau,n}=\int_{\Gamma_C}\frac{1}{2\gamma_h}\left(\left[\mathrm{P}^{n+1}\right]_{\mathbb{R}^-}\left[\mathrm{P}^{n}\right]_{\mathbb{R}^+}-\left[\mathrm{P}^{n}\right]_{\mathbb{R}^-}\left[\mathrm{P}^{n+1}\right]_{\mathbb{R}^+}\right)\,d\Gamma.$$

We note that $\left[\mathrm{P}^{n+1}\right]_{\mathbb{R}^-}\left[\mathrm{P}^{n}\right]_{\mathbb{R}^+} \leq 0$ and use $-\left[\mathrm{P}^{n}\right]_{\mathbb{R}^-}\left[\mathrm{P}^{n+1}\right]_{\mathbb{R}^+} \leq \frac{1}{4}(\left[\mathrm{P}^{n+1}\right]_{\mathbb{R}^+}-\left[\mathrm{P}^{n}\right]_{\mathbb{R}^-})^2 \leq \frac{1}{4}(\mathrm{P}^{n+1}-\mathrm{P}^{n})^2$ to get:

$$E^{h,\tau,n+1}-E^{h,\tau,n}\leq\int_{\Gamma_C}\frac{1}{8\gamma_h}(\mathrm{P}^{n+1}-\mathrm{P}^{n})^2\,d\Gamma.$$

Since the mesh is quasi-uniform, we then use Lemma 2.3, the trace inequality of [6, Theorem 1.6.6] and the inverse inequality [25, Corollary 1.141, Remark 1.143] to obtain, for γ_0 large enough

$$\begin{aligned}
E^{h,\tau,n+1} - E^{h,\tau,n} &\leq \int_{\Gamma_C} \frac{1}{8\gamma_h}(\sigma_n(\mathbf{u}^{h,n+1} - \mathbf{u}^{h,n}) - \gamma_h u_n^{h,n+1} + \gamma_h u_n^{h,n})^2 d\Gamma \\
&\leq C\left(\frac{1}{\gamma_0}\|\sigma_n(\mathbf{u}^{h,n+1} - \mathbf{u}^{h,n})\|^2_{-\frac{1}{2},h,\Gamma_C} + \gamma_0 \|u_n^{h,n+1} - u_n^{h,n}\|^2_{\frac{1}{2},h,\Gamma_C}\right) \\
&\leq C\left(\|\mathbf{u}^{h,n+1} - \mathbf{u}^{h,n}\|^2_{1,\Omega} + \frac{\gamma_0}{h}\|\mathbf{u}^{h,n+1} - \mathbf{u}^{h,n}\|_{1,\Omega}\|\mathbf{u}^{h,n+1} - \mathbf{u}^{h,n}\|_{0,\Omega}\right) \\
&\leq C\frac{\gamma_0}{h^2}\|\mathbf{u}^{h,n+1} - \mathbf{u}^{h,n}\|^2_{0,\Omega} = C\frac{\gamma_0}{h^2}\|\tau\dot{\mathbf{u}}^{h,n} + \frac{\tau^2}{2}\ddot{\mathbf{u}}^{h,n}\|^2_{0,\Omega} \\
&\leq C\gamma_0\left(\frac{\tau^2}{h^2}\|\dot{\mathbf{u}}^{h,n}\|^2_{0,\Omega} + \frac{\tau^4}{h^2}\|\ddot{\mathbf{u}}^{h,n}\|^2_{0,\Omega}\right).
\end{aligned}$$

Following exactly the same path as above, but using $\|\cdot\|_{0,\Omega} \leq \|\cdot\|_{1,\Omega}$ after the trace inequality, we bound also:

$$\|[\mathrm{P}^{\mathbf{n}}_{1,\gamma_h}(\mathbf{u}^{h,n})]_{\mathbb{R}^-}\|^2_{-\frac{1}{2},h,\Gamma_C} \leq C\frac{\gamma_0^2}{h}\|\mathbf{u}^{h,n}\|^2_{1,\Omega}.$$

We combine the above result with the bound (18). This yields:

$$\|\ddot{\mathbf{u}}^{h,n}\|_{0,\Omega} \leq \frac{C}{h}(\|\mathbf{u}^{h,n}\|_{1,\Omega} + \|[\mathrm{P}^{\mathbf{n}}_{1,\gamma_h}(\mathbf{u}^{h,n})]_{\mathbb{R}^-}\|_{-\frac{1}{2},h,\Gamma_C}) \leq \frac{C\gamma_0}{h^{\frac{3}{2}}}\|\mathbf{u}^{h,n}\|_{1,\Omega}.$$

This results into:

$$E^{h,\tau,n+1} - E^{h,\tau,n} \leq \; C\gamma_0\left(\frac{\tau^2}{h^2}\|\dot{\mathbf{u}}^{h,n}\|^2_{0,\Omega} + \frac{\gamma_0^2\tau^4}{h^5}\|\mathbf{u}^{h,n}\|^2_{1,\Omega}\right),$$

from which we can deduce, using Proposition 3.2:

$$E^{h,\tau,n+1} \leq \left(1 + C\gamma_0\frac{\tau^2}{h^2}\left(1 + \frac{\gamma_0^2\tau^2}{h^3}\right)\right)E^{h,\tau,n}.$$

This means that, still with $N = \frac{T}{\tau}$,

$$\begin{aligned}
E^{h,\tau,N} &\leq \left(1 + C\gamma_0\frac{\tau^2}{h^2}\left(1 + \frac{\gamma_0^2\tau^2}{h^3}\right)\right)^N E^{h,\tau,0} \\
&\leq e^{CN\gamma_0\frac{\tau^2}{h^2}\left(1+\frac{\gamma_0^2\tau^2}{h^3}\right)}E^{h,\tau,0} \\
&= e^{CT\frac{\gamma_0\tau}{h^2}\left(1+\frac{\gamma_0^2\tau^2}{h^3}\right)}E^{h,\tau,0},
\end{aligned}$$

which remains bounded under the assumption (22). The boundedness of $E^{h,N}$ is then deduced from Proposition 3.2. □

3.4 Comments on the stability analysis

The stability result given by Proposition 3.8 is submitted to a CFL condition $\tau = \mathcal{O}(h^2)$. Of course, this is not the expected one which would be $\tau = \mathcal{O}(h)$ in accordance with the result of

Proposition 3.2 and the stability analysis of Verlet scheme for a linear evolution equation (see, e.g., [16]). The reason of the non-optimality of Proposition 3.8 is that we did not succeed to optimally bound the involved contact term $\left(\left[\mathrm{P}^{n+1}\right]_{\mathbb{R}^-}\left[\mathrm{P}^{n}\right]_{\mathbb{R}^+} - \left[\mathrm{P}^{n}\right]_{\mathbb{R}^-}\left[\mathrm{P}^{n+1}\right]_{\mathbb{R}^+}\right)$. However, an important remark is that this term vanishes unless the terms P^n and P^{n+1} are of opposite signs, which occurs only when the contact status changes. Moreover it is positive only when the status changes from contact to non-contact. If we assume that the number of such transitions is finite during the simulation, a stability result with a condition $\tau = \mathcal{O}(h)$ may be recovered. However, an infinite number of changes of the contact status cannot be excluded. Another argument in favor of such a stability result is obtained via the definition of the following linear (but depending on $\mathbf{u}^{h,n}$) operator $\mathbf{B}^{h,n} : \mathbf{V}^h \to \mathbf{V}^h$:

$$(\mathbf{B}^{h,n}\mathbf{v}^h, \mathbf{w}^h)_{\gamma_h} = A_{\Theta\gamma_h}(\mathbf{v}^h, \mathbf{w}^h) + \int_{\Gamma_C} \frac{1}{\gamma_h} H\left(-\mathrm{P}^{\mathbf{n}}_{1,\gamma_h}(\mathbf{u}^{h,n})\right) \mathrm{P}^{\mathbf{n}}_{1,\gamma_h}(\mathbf{v}^h)\mathrm{P}^{\mathbf{n}}_{\Theta,\gamma_h}(\mathbf{w}^h)d\Gamma,$$

for all $\mathbf{v}^h, \mathbf{w}^h \in \mathbf{V}^h$. Due to the relationship $[x]_{\mathbb{R}^-} = H(-x)\,x$ for $x \in \mathbb{R}$, there holds:

$$\begin{aligned}
(\mathbf{B}^h\mathbf{u}^{h,n}, \mathbf{w}^h)_{\gamma_h} &= A^{\mathbf{n}}_{\Theta\gamma_h}(\mathbf{u}^{h,n}, \mathbf{w}^h) + \int_{\Gamma_C} \frac{1}{\gamma_h} \left[\mathrm{P}^{\mathbf{n}}_{1,\gamma_h}(\mathbf{u}^{h,n})\right]_{\mathbb{R}^-} \mathrm{P}^{\mathbf{n}}_{\Theta,\gamma_h}(\mathbf{w}^h)\, d\Gamma \\
&= A^{\mathbf{n}}_{\Theta\gamma_h}(\mathbf{u}^{h,n}, \mathbf{w}^h) + \int_{\Gamma_C} \frac{1}{\gamma_h} H(-\mathrm{P}^{\mathbf{n}}_{1,\gamma_h}(\mathbf{u}^{h,n}))\mathrm{P}^{\mathbf{n}}_{1,\gamma_h}(\mathbf{u}^{h,n})\mathrm{P}^{\mathbf{n}}_{\Theta,\gamma_h}(\mathbf{w}^h)\, d\Gamma \\
&= (\mathbf{B}^{h,n}\mathbf{u}^{h,n}, \mathbf{w}^h)_{\gamma_h}
\end{aligned}$$

for all $\mathbf{w}^h \in \mathbf{V}^h$, and therefore

$$\mathbf{B}^{h,n}\mathbf{u}^{h,n} = \mathbf{B}^h\mathbf{u}^{h,n}.$$

The following bound on the norm of $\mathbf{B}^{h,n}$ can be established, following an argument similar to [11, Theorem 2.8]:

Lemma 3.9. *Let us suppose that γ_0 is large enough. There exists a constant $C > 0$, independent of Θ, γ_0 and h, such that*

$$\|\mathbf{B}^{h,n}\|_{\gamma_h} \leq C(1 + |\Theta|), \tag{23}$$

where $\|\cdot\|_{\gamma_h}$ is the operator norm induced by the norm $\|\cdot\|_{\gamma_h}$ on $\mathbf{V}^h$.

Proof. Let us take $\mathbf{v}^h$ and $\mathbf{w}^h$ in $\mathbf{V}^h$. First, using Lemma 2.3 there holds

$$\|\mathrm{P}^{\mathbf{n}}_{\Theta,\gamma_h}(\mathbf{w}^h)\|_{0,\Gamma_C} \leq \left(\|\gamma_h{}^{\frac{1}{2}} w^h_n\|_{0,\Gamma} + C|\Theta|\|\mathbf{w}^h\|_{1,\Omega}\right) \leq C(1 + |\Theta|)\|\mathbf{w}^h\|_{\gamma_h},$$

and the same bound holds for $\|\mathrm{P}^{\mathbf{n}}_{1,\gamma_h}(\mathbf{v}^h)\|_{0,\Gamma_C}$, replacing $|\Theta|$ by 1. Then, using Lemma 2.3 and the above result, we bound:

$$\begin{aligned}
&|(\mathbf{B}^{h,n}\mathbf{v}^h, \mathbf{w}^h)_{\gamma_h}| \\
\leq\, &C(1 + |\Theta|)\|\mathbf{v}^h\|_{1,\Omega}\|\mathbf{w}^h\|_{1,\Omega} + \|\mathrm{P}^{\mathbf{n}}_{1,\gamma_h}(\mathbf{v}^h)\|_{0,\Gamma_C}\|\mathrm{P}^{\mathbf{n}}_{\Theta,\gamma_h}(\mathbf{w}^h)\|_{0,\Gamma_C} \\
\leq\, &C(1 + |\Theta|)\|\mathbf{v}^h\|_{\gamma_h}\|\mathbf{w}^h\|_{\gamma_h},
\end{aligned}$$

which proves the assertion (23). □

Using $\mathbf{B}^{h,n}$ we can rewrite the operator associated to the scheme (13) as:

$$\mathbf{C}^{h,n} = \begin{bmatrix} 2\mathbf{I} - \tau^2(\mathbf{M}^h)^{-1}\mathbf{B}^{h,n} & -\mathbf{I} \\ \mathbf{I} & \mathbf{0} \end{bmatrix},$$

where $\mathbf{I}$ is the identity operator. It links the successive values $\mathbf{u}^{h,n+1}, \mathbf{u}^{h,n}$ and $\mathbf{u}^{h,n-1}$ thanks to

$$\begin{bmatrix} \mathbf{u}^{h,n+1} \\ \mathbf{u}^{h,n} \end{bmatrix} = \mathbf{C}^{h,n} \begin{bmatrix} \mathbf{u}^{h,n} \\ \mathbf{u}^{h,n-1} \end{bmatrix},$$

when neglecting the source term $\mathbf{L}^{h,n}$. For a linear problem this would correspond to the amplification matrix. The following result can be established for $\mathbf{C}^{h,n}$:

Proposition 3.10. *Let us suppose that the mesh $\mathcal{T}^h$ is quasi-uniform, that γ_0 is large and*

$$\gamma_0^{\frac{1}{2}} \tau \leq Ch,$$

where $C > 0$ is a constant independent of γ_0, h and τ. Then, $\mathbf{C}^{h,n}$ is diagonalizable and its spectral radius $\rho(\mathbf{C}^{h,n})$ is equal to 1. Furthermore, the same conclusion holds for $\mathbf{C}^{h,n}\mathbf{C}^{h,n+1}$, which is diagonalizable with a spectral radius $\rho(\mathbf{C}^{h,n}\mathbf{C}^{h,n+1})$ also equal to 1.

Proof. Let us consider $\lambda \in \mathbb{C}$ an eigenvalue of the operator $\mathbf{C}^{h,n}$. Denoting $\mathbf{A}^{h,n} = 2\mathbf{I} - \tau^2(\mathbf{M}^h)^{-1}\mathbf{B}^{h,n}$, this means there exists a non-zero pair $(\mathbf{v}^h, \mathbf{w}^h) \in \mathbf{V}^h \times \mathbf{V}^h$ such that:

$$\begin{aligned} \mathbf{A}^{h,n}\mathbf{v}^h - \mathbf{w}^h &= \lambda \mathbf{v}^h \\ \mathbf{v}^h &= \lambda \mathbf{w}^h. \end{aligned}$$

With help of the second equation, the first one can be written $\lambda \mathbf{A}^{h,n}\mathbf{w}^h - \mathbf{w}^h = \lambda^2 \mathbf{w}^h$, or equivalently

$$\mathbf{A}^{h,n}\mathbf{w}^h = \frac{1+\lambda^2}{\lambda}\mathbf{w}^h. \tag{24}$$

We then use [11, Lemma A.1] and Lemma 3.9 to bound

$$\|(\mathbf{M}^h)^{-1}\mathbf{B}^{h,n}\|_{\gamma_h} \leq \|(\mathbf{M}^h)^{-1}\|_{\gamma_h} \|\mathbf{B}^{h,n}\|_{\gamma_h} \leq C(1+|\Theta|)\frac{\gamma_0}{h^2}.$$

We now consider $\gamma_0^{\frac{1}{2}}\tau/h$ small enough so that the eigenvalues of $\mathbf{A}^{h,n} = (2\mathbf{I} - \tau^2(\mathbf{M}^h)^{-1}\mathbf{B}^{h,n})$ are positive. We call α_j these eigenvalues and $\mathbf{w}_j^h$ the corresponding eigenvectors. Taking $\mathbf{w}^h = \mathbf{w}_j^h$ in equation (24), we deduce that, for each index j, we can compute two eigenvalues $\lambda_j^{\pm}$ which are solution to

$$\lambda^2 - \alpha_j \lambda + 1 = 0.$$

Since the eigenvalues of $(\mathbf{M}^h)^{-1}\mathbf{B}^{h,n}$ are all positive, we infer $\alpha_j < 2$, and $\Delta_j = \alpha_j^2 - 4 < 0$. Therefore the above algebraic equation has two imaginary solutions

$$\lambda_j^{\pm} = \frac{\alpha_j \pm i\sqrt{-\Delta_j}}{2}.$$

Remark that these eigenvalues are such that

$$|\lambda_j^{\pm}| = \frac{1}{4}(\alpha_j^2 + 4 - \alpha_j^2) = 1.$$

This allows to conclude that $\mathbf{C}^{h,n}$ is diagonalizable and $\rho(\mathbf{C}^{h,n}) = 1$. We can now make a similar computation for two successive iterations. Since

$$\mathbf{C}^{h,n+1}\mathbf{C}^{h,n} = \begin{bmatrix} \mathbf{A}^{h,n+1}\mathbf{A}^{h,n} - \mathbf{I} & -\mathbf{A}^{h,n+1} \\ \mathbf{A}^{h,n} & -\mathbf{I} \end{bmatrix},$$

$\lambda \in \mathbb{C}$ is an eigenvalue of $\mathbf{C}^{h,n+1}\mathbf{C}^{h,n}$ if there exists a non-zero pair $(\mathbf{v}^h, \mathbf{w}^h) \in \mathbf{V}^h \times \mathbf{V}^h$ verifying:

$$\begin{aligned} \mathbf{A}^{h,n+1}\mathbf{A}^{h,n}\mathbf{v}^h - \mathbf{v}^h - \mathbf{A}^{h,n+1}\mathbf{w}^h &= \lambda \mathbf{v}^h, \\ \mathbf{A}^{h,n}\mathbf{v}^h - \mathbf{w}^h &= \lambda \mathbf{w}^h, \end{aligned}$$

which implies

$$\lambda \mathbf{A}^{h,n+1}\mathbf{A}^{h,n}\mathbf{v}^h = (\lambda+1)^2 \mathbf{v}^h.$$

If we denote by β_j the eigenvalues of $\mathbf{A}^{h,n+1}\mathbf{A}^{h,n}$ which are close to 4 for $\gamma_0^{\frac{1}{2}}\tau/h$ small enough, and $\mathbf{v}_j^h$ the corresponding eigenvectors, we conclude that the eigenvalues of $\mathbf{C}^{h,n+1}\mathbf{C}^{h,n}$ are

$$\lambda_j^{\pm} = \frac{(2-\beta_j) \pm i\sqrt{4-(\beta_j-2)^2}}{2}.$$

Since $|\lambda_j^{\pm}| = 1$, the operator $\mathbf{C}^{h,n+1}\mathbf{C}^{h,n}$ is diagonalizable with a unit spectral radius. □

Remark 3.11. *For a linear problem, we would conclude that the scheme is stable, under the condition $\frac{\tau}{h}$ small enough. However, in a nonlinear framework, the conclusion cannot be drawn since the matrix $\mathbf{C}^{h,n}$ changes from an iteration to another. Moreover, it seems difficult to pursue the reasoning made on two iterations to an arbitrary number of iterations.*

4 Numerical experiments

We first carry out numerical experiments in 1D, where we can compare our results with an exact solution. Then, numerical experiments in 2D/3D will be described. These numerical tests are performed with the help of our freely available finite element library GetFEM++ (see `http://getfem.org`).

4.1 1D numerical experiments: multiple impacts of an elastic bar

We first present the setting, and then the results obtained by combination of Nitsche's contact discretization and Verlet scheme. These results are also compared with computations using other methods: the Paoli-Schatzman scheme, the Taylor-Flanagan scheme, the mass redistribution method and the penalty method. This section is ended with numerical convergence tests.

4.1.1 Setting

We first deal with the one-dimensional case $d = 1$ with a single contact point, namely an elastic bar $\Omega = (0, L)$ with $\Gamma_C = \{0\}$, $\Gamma_D = \{L\}$ and $\Gamma_N = \emptyset$. The elastodynamic equation is then reduced to find $u : \Omega_T = (0,T) \times (0,L) \to \mathbb{R}$ such that:

$$\rho \ddot{u} - E\frac{\partial^2 u}{\partial x^2} = f, \qquad \text{in } \Omega_T, \tag{25}$$

where E is the Young modulus and the Cauchy stress tensor is given by $\sigma(u) = E(\partial u/\partial x)$. Note that $\sigma_n(u) = (\sigma(u)n)\cdot n = \sigma(u)$ on Γ_C. In this case, problem (1)–(2) admits one unique solution (see e.g. [18]) for which the following energy conservation equation holds, for t a.e. in $(0,T)$:

$$\frac{1}{2}\frac{d}{dt}\left(\int_\Omega \rho \dot{u}^2(t)d\Omega + \int_\Omega E\left(\frac{\partial u}{\partial x}(t)\right)^2 d\Omega\right) = -\int_\Omega f(t)\dot{u}(t)d\Omega. \tag{26}$$

We consider a finite element space using linear ($k = 1$) or quadratic ($k = 2$) finite elements and a uniform subdivision of $[0, L]$ with M segments (so $L = Mh$). We denote the vector which contains all the nodal values of $\mathbf{u}^{h,n}$ (resp. $\dot{\mathbf{u}}^{h,n}$ and $\ddot{\mathbf{u}}^{h,n}$) by $\mathbf{U}^n := [U_0^n, \ldots, U_N^n]^T$ (resp. $\dot{\mathbf{U}}^n$, $\ddot{\mathbf{U}}^n$). The component of index 0 corresponds to the node at the contact point Γ_C. We also note $\mathbf{M}$, resp. $\mathbf{K}$, the mass, resp. the stiffness, matrix that results from the finite element discretization. We introduce the Courant number which is defined as:

$$\nu_C := c_0 \frac{\tau}{h} = \sqrt{\frac{E}{\rho}} \frac{\tau}{h},$$

where c_0 is the wave speed associated to the bar. For each simulation, we compute and plot the following time-dependent quantities:

1. The displacement u at the contact point Γ_C, given at time t^n by $u^{h,n}(0) (= U_0^n)$.

2. The contact pressure σ_C, which, in the discrete case, is different from $\sigma(u)$. If a standard (mixed) method is used for the treatment of contact, it is directly given by the Lagrange multiplier, i.e., $\sigma_C^n := \lambda^{h,n}$ at time t^n. In the case of the Nitsche-based formulation, it can be computed as follows at time t^n:

$$\sigma_C^n := \left[\sigma_n(u^{h,n})(0) - \gamma_h(-u^{h,n}(0))\right]_{\mathbb{R}^-} = \left[\frac{E}{h}(U_1^n - U_0^n) + \frac{\gamma_0}{h} U_0^n\right]_{\mathbb{R}^-},$$

   which comes from the contact condition (7).

3. The discrete energy E^h which is at time t^n

$$E^{h,n} = \frac{1}{2}\left((\dot{\mathbf{U}}^n)^{\mathrm{T}} \mathbf{M} \dot{\mathbf{U}}^n + (\mathbf{U}^n)^{\mathrm{T}} \mathbf{K} \mathbf{U}^n\right),$$

   and the discrete augmented energy E_1^h:

$$E_1^{h,n} = E^{h,n} - R^{h,n}, \quad R^{h,n} = \frac{h}{2\gamma_0}\left((\sigma_n(u^{h,n})(0))^2 - (\sigma_C^n)^2\right).$$

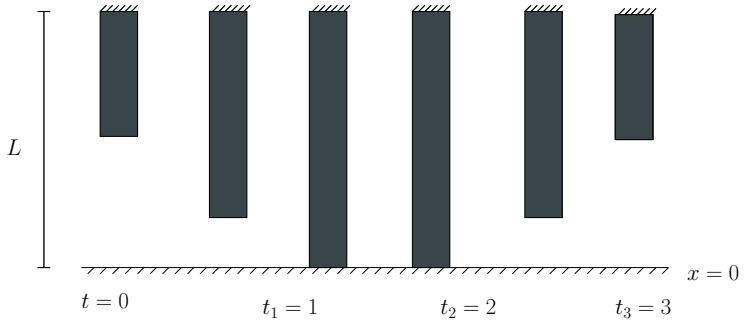

Figure 1: Multiple impacts of an elastic bar. The bar is clamped at $x = L$ and the contact node is located at the bottom. The closed-form solution is periodic of period 3, with one impact during each period (here between $t = 1$ and $t = 2$).

We propose a benchmark associated to multiple impacts. This allows to check both the presence of spurious oscillations and the long term energetic behavior of the method. In the absence of external volume forces, the bar is initially compressed. Then, it is released without initial velocity. It impacts first the rigid ground, located at $x = 0$, and then gets compressed again. We take the following values for the parameters: $f = 0$, $E = 1$, $\rho = 1$, $L = 1$, $u_0(x) = \frac{1}{2} - \frac{x}{2}$ and $\dot{u}_0(x) = 0$. This problem admits a closed-form solution u which derivation and expression is detailed in [19]. Notably, it has a periodic motion of period 3. At each period, the bar stays in contact with the rigid ground during one time unit (see Figure 1). The chosen simulation time is $T = 12$, so that we can observe 4 successive impacts.

4.1.2 Numerical results for Nitsche's method

We discretize the bar with $M = 20$ linear finite elements ($k = 1$, $h = 0.05$) and take $\tau = 0.01$. The resulting Courant number is $\nu_C = 0.2$. Note that almost all the parameters have been taken identical as in [12] for comparison purposes. The number of element is smaller ($M = 20$ instead of 100 in [12]) and the time-step τ is 0.01 for stability reasons. We first investigate the variant $\Theta = 0$ with a parameter $\gamma_0 = 1$. The mass matrix is computed in a standard fashion. The choice γ_0 equal to 1 is guided by the concern to obtain a stiffness associated with the degree of freedom on the contact boundary comparable to the stiffnesses obtained by the finite element discretization inside the bar.

The results are depicted in Figure 2 where the approximated solution corresponds to the solid blue line and the red dotted line is the exact solution. Note also that the dashed energy is E_1^h, the modified energy given by expression (11).

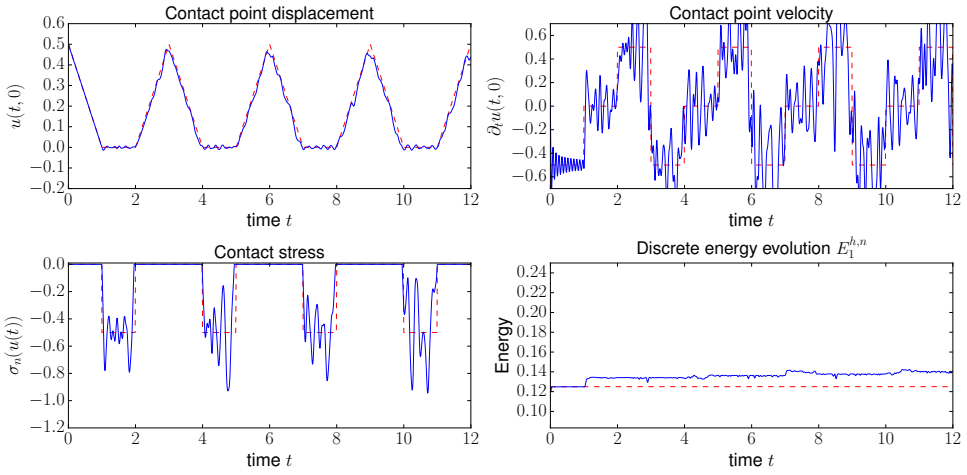

Figure 2: Multiple impacts of an elastic bar. Nitsche's method with Verlet scheme for $h = 1/20$, $\tau = 0.01$, $\Theta = 0$, $\gamma_0 = 1$ and P_1 Lagrange finite elements.

For an element size which remains relatively rough, one notes the good approximation of the displacement. Significant oscillations can be deplored on the velocity of the contact point, but unfortunately they are very difficult to avoid. Indeed, since a velocity shock is propagating without attenuation or dissipation in the proposed test case, the Gibbs phenomena are inevitable in the finite element approximation. It would be the case even without a contact condition. The approximation of the contact stress is, although polluted by oscillations too, of good quality given the discontinuous character of the exact solution and the relatively coarse mesh size (one

can compare with the results obtained in [12] for elements five times smaller). The evolution of the energy reveals some variations which are far from being negligible, but remain moderate, and without appearance of instabilities. Moreover these variations tend to decrease for a finer element size.

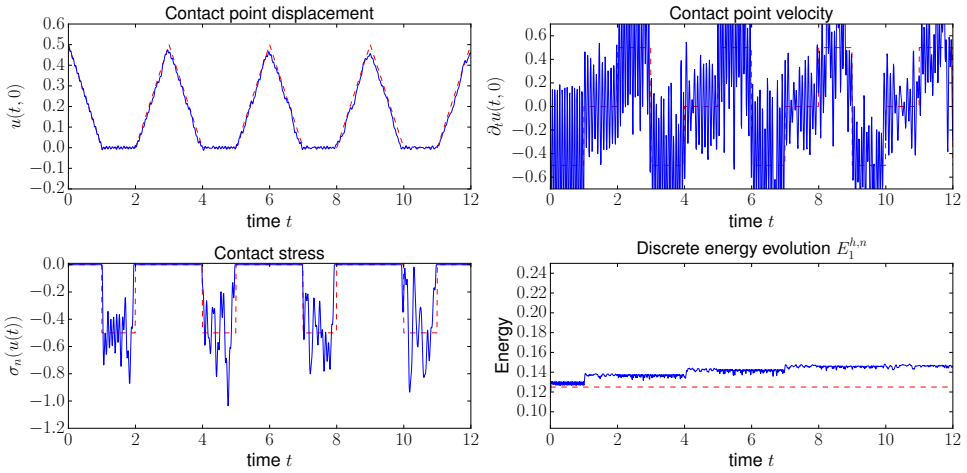

Figure 3: Multiple impacts of an elastic bar. Nitsche's method with Verlet scheme for $h = 1/20$, $\tau = 0.01$, $\Theta = -1$, $\gamma_0 = 1$ and P_1 Lagrange finite elements.

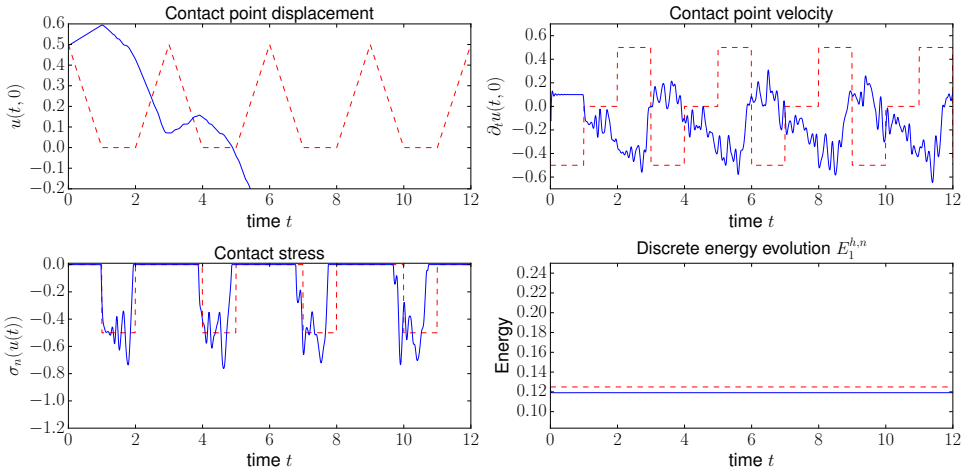

Figure 4: Multiple impacts of an elastic bar. Nitsche's method with Verlet scheme for $h = 1/20$, $\tau = 0.01$, $\Theta = 1$, $\gamma_0 = 1$ and P_1 Lagrange finite elements.

The calculation for the variant $\Theta = -1$ and for Nitsche's parameter γ_0 still equal to 1 is presented on Figure 3. It can be seen that the non-penetration condition is slightly better respected, which indicates that the additional terms compared to the variant $\Theta = 0$ reinforce the consistency of the method. However, this is at the price of stronger oscillations on the velocity at the contact point. The approximation of the contact stress remains comparable to the $\Theta = 0$ variant, as well as the energy evolution.

For the same test with the variant $\Theta = 1$ and Nitsche's parameter $\gamma_0 = 1$, as shown in Figure 4, one gets a non convergent approximation of the displacement. This is due to the loss

of coercivity arising when the assumption of Proposition 3.1 is not satisfied. Indeed, the variant $\Theta = 1$ is the most restrictive from this point of view and needs a larger parameter γ_0. Figure 5 represents the simulation for $\gamma_0 = 2$ which allows to recover the coercivity. We observe the very good conservation of the discrete energy together with a good approximation of the non-penetration condition. The level of oscillations on the contact point velocity and on the contact stress is similar with the case $\Theta = 0$.

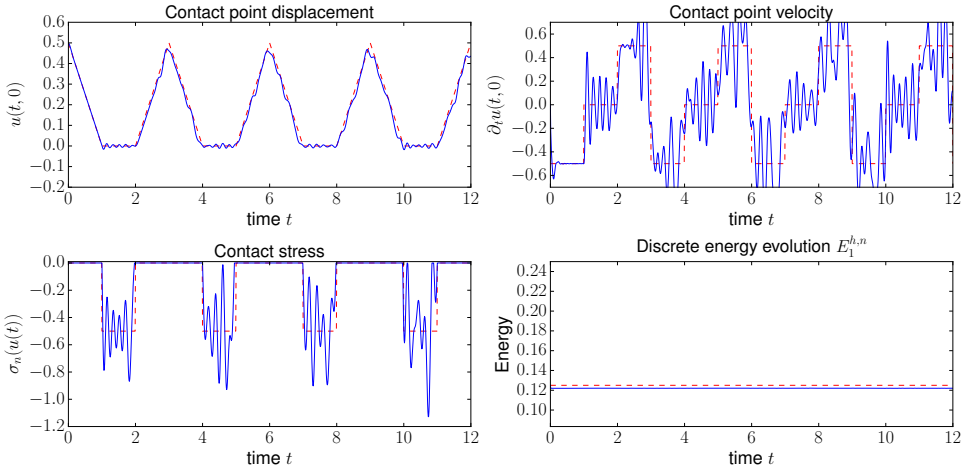

Figure 5: Multiple impacts of an elastic bar. Nitsche's method with Verlet scheme for $h = 1/20$, $\tau = 0.01$, $\Theta = 1$, $\gamma_0 = 2$ and P_1 Lagrange finite elements.

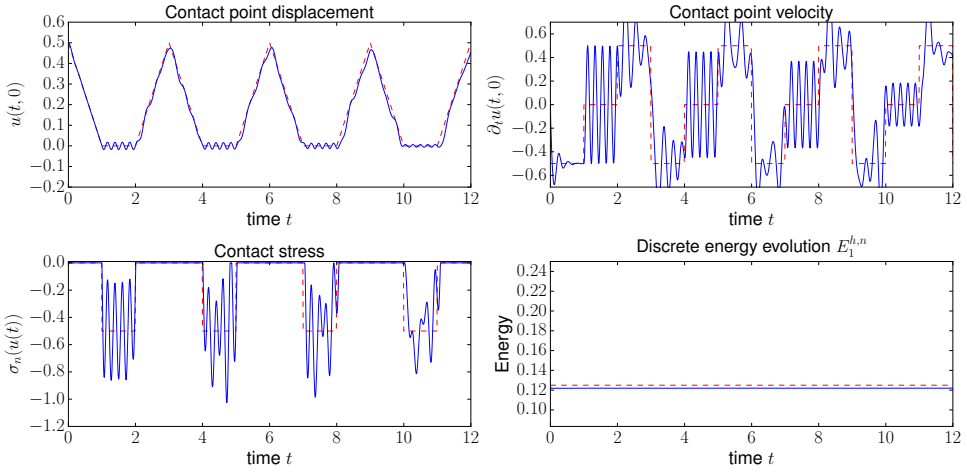

Figure 6: Multiple impacts of an elastic bar. Nitsche's method with Verlet scheme for $h = 1/20$, $\tau = 0.01$, $\Theta = 1$, $\gamma_0 = 2$, P_1 Lagrange finite elements and a lumped mass matrix.

Finally, Figure 6 displays a simulation still for ($\Theta = 1$, $\gamma_0 = 2$) but using a lumped mass matrix. Following a standard strategy for P_1 Lagrange finite elements, on each row, the extra-diagonal components of the mass matrix are set to zero and added to the diagonal component. The comparison with Figure 5 allows to notice more pronounced oscillations on the displacement, the velocity and the contact stress, but still with a very good energy conservation.

4.1.3 Comparison with Paoli-Schatzman scheme

The Paoli-Schatzman scheme directly addresses the measure differential inclusion that results from the finite element semi–discretization of the dynamic contact problem. Following [39, 40, 41, 42, 43], it can be summarized as follows. Let $\mathcal{U}^h_{adm}$ be the approximated set of admissible displacements such that $\mathbf{U} \in \mathcal{U}^h_{adm}$ means that the vector of degrees of freedom $\mathbf{U}$ satisfies a chosen approximated non-penetration condition. In our one-dimensional test case, this can be simply written $U_0 \geq 0$, where U_0 is the displacement of the contact point. Then, still denoting $\mathbf{M}$, resp. $\mathbf{K}$, the mass, resp. stiffness, matrices that result from the finite element discretization, the (generally ill-posed) measure differential inclusion resulting from the semi–discretization of the dynamic contact problem (1)–(2) can be written:

$$\ddot{\mathbf{U}}(t) + \mathbf{M}^{-1}\mathbf{K}\mathbf{U}(t) + \partial I_{\mathcal{U}^h_{adm}}(\mathbf{U}(t)) \ni \mathbf{M}^{-1}\mathbf{L}(t),$$

where $\partial I_{\mathcal{U}^h_{adm}}(\mathbf{U})$ denotes the normal cone to $\mathcal{U}^h_{adm}$ at $\mathbf{U}$. Then, the Paoli-Schatzman scheme can be written for a given restitution coefficient $e \in [0, 1]$:

$$\left(\frac{\mathbf{U}^{n+1} - 2\mathbf{U}^n + \mathbf{U}^{n-1}}{\tau^2}\right) + \mathbf{M}^{-1}\mathbf{K}\mathbf{U}^n + \partial I_{\mathcal{U}^h_{adm}}\left(\frac{\mathbf{U}^{n+1} + e\mathbf{U}^{n-1}}{1+e}\right) \ni \mathbf{M}^{-1}\mathbf{L}^n.$$

Of course, one easily recognize the Verlet scheme except for the contact constraint which is taken in an implicit manner and prescribed to the intermediate displacement $\mathbf{U}^{n+1,e} = \dfrac{\mathbf{U}^{n+1} + e\mathbf{U}^{n-1}}{1+e}$.

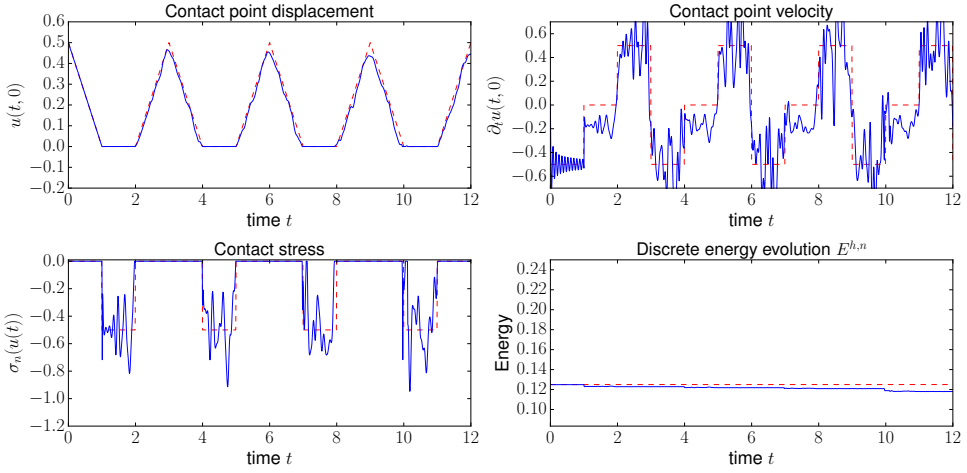

Figure 7: Multiple impacts of an elastic bar. Paoli-Schatzman scheme for $h = 1/20$, $\tau = 0.01$, $e = 0$ and P_1 Lagrange finite elements.

When implementation is considered, one usually introduces a multiplier to prescribe the constraint. Denoting by $\mathbf{B}$ the matrix having N_c lines such that the non-penetration condition reads $(\mathbf{B}\mathbf{U})_i \leq 0, \quad i = 1 \cdots N_c$, the scheme may be re-written

$$\left(\frac{\mathbf{U}^{n+1} - 2\mathbf{U}^n + \mathbf{U}^{n-1}}{\tau^2}\right) + \mathbf{M}^{-1}\mathbf{K}\mathbf{U}^n + \mathbf{B}^{\mathrm{T}}\Lambda^{n+1} = \mathbf{M}^{-1}\mathbf{L}^n, \tag{27}$$

$$\left(\mathbf{B}\mathbf{U}^{n+1,e}\right)_i \leq 0, \quad \Lambda_i^{n+1} \leq 0, \quad \left(\mathbf{B}\mathbf{U}^{n+1,e}\right)_i \Lambda_i^{n+1} = 0, \quad i = 1 \cdots N_c, \tag{28}$$

or, as a one–step scheme

$$\mathbf{U}^{n+1} = \mathbf{U}^n + \tau\dot{\mathbf{U}}^n - \frac{\tau^2}{2}\mathbf{M}^{-1}(\mathbf{K}\mathbf{U}^n - \mathbf{L}^n) - \frac{\tau^2}{2}\mathbf{B}^{\mathrm{T}}\Lambda^{n+1}, \tag{29}$$

$$\dot{\mathbf{U}}^{n+1} = \dot{\mathbf{U}}^n - \frac{\tau}{2}\mathbf{M}^{-1}(\mathbf{K}\mathbf{U}^n - \mathbf{L}^n + \mathbf{K}\mathbf{U}^{n+1} - \mathbf{L}^{n+1}) - \tau\mathbf{B}^{\mathrm{T}}\Lambda^{n+1}, \tag{30}$$

still with the addition of the complementarity conditions (28). The proof that the restitution coefficient e is asymptotically reached for a vanishing time–step is detailed in [41, 42].

Note that, even though Verlet scheme is an explicit scheme, the implicitation of the contact force in Paoli-Schatzman scheme results in a global problem to be solved on the contact surface at each time–step. Of course, this corresponds to a scalar algebraic equation which can be explicitly solved in the one-dimensional test.

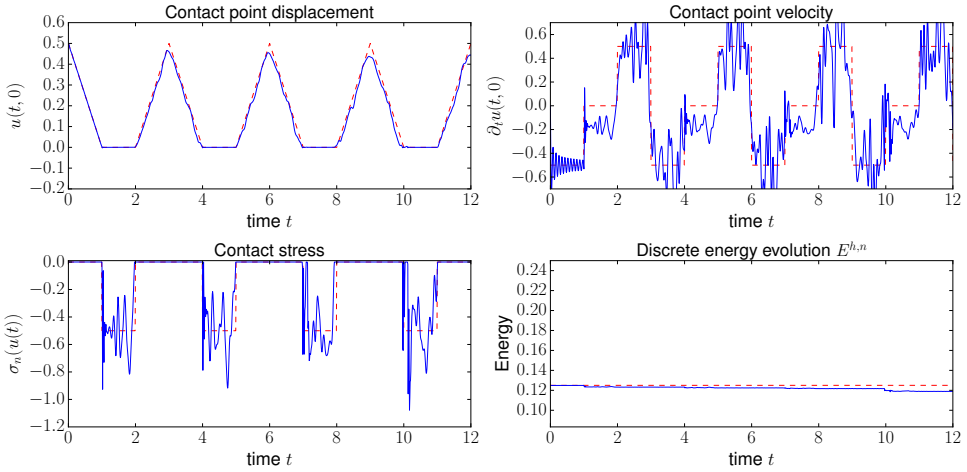

Figure 8: Multiple impacts of an elastic bar. Paoli-Schatzman scheme for $h = 1/20$, $\tau = 0.01$, $e = 1/2$ and P_1 Lagrange finite elements.

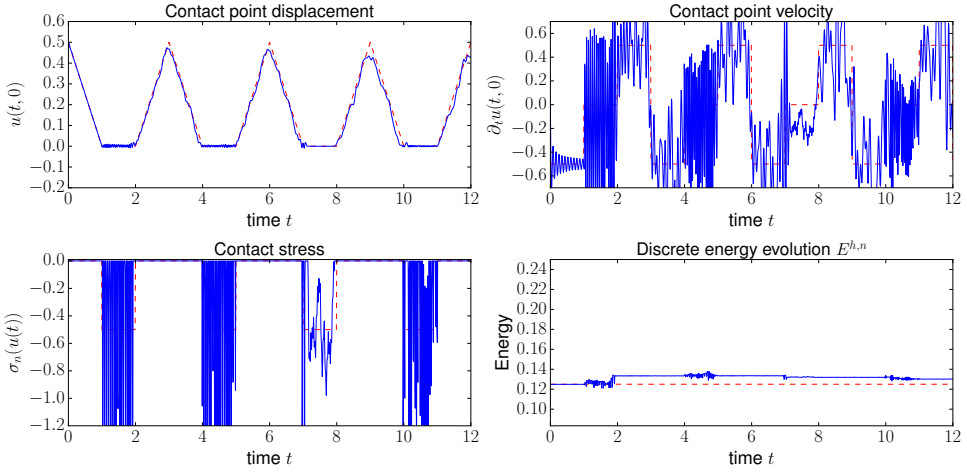

Figure 9: Multiple impacts of an elastic bar. Paoli-Schatzman scheme for $h = 1/20$, $\tau = 0.01$, $e = 1$ and P_1 Lagrange finite elements.

The numerical tests for $h = 0.05$ and $\tau = 0.01$ are presented in figures 7, 8 and 9 for a restitution coefficient equal to 0, 1/2 and 1, respectively. The results for $e = 0$ and $e = 1/2$ are very similar to each other despite the difference between the restitution coefficients, and we observe a very similar loss of energy for each impact. The approximation of the displacement and of the non-penetration condition are quite good. The results for $e = 1$ show an excessive bounce of the contact point which leads to very noisy contact point velocity and contact stress.

4.1.4 Comparison with Taylor-Flanagan scheme

L.M. Taylor and D.P. Flanagan [52] developed an explicit scheme in the framework of PRONTO3D software which rapidly became a reference for explicit integration of contact and impact problems. To summarize the principle of the method, it is based on the Leapfrog form of Verlet scheme (16). When contact occurs, the persistency condition is prescribed at the half time–step by enforcing the relative velocity to vanish (see Equation (21) in [29], for instance). To this aim, a Lagrange multiplier is introduced which is taken into account in an implicit way. The equation associated to the Lagrange multiplier can be solved locally only in a node-to-node contact approximation. For a more general contact condition, the Lagrange multiplier is obtained by solving a global problem on the contact surface. However, Taylor and Flanagan propose an iterative method to compute the Lagrange multiplier which needs only a few iterations.

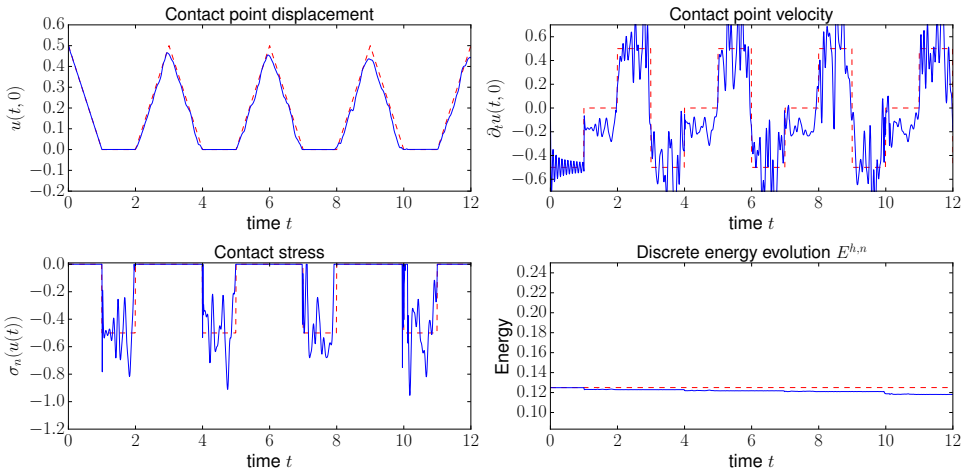

Figure 10: Multiple impacts of an elastic bar. Taylor-Flanagan scheme for $h = 1/20$, $\tau = 0.01$, and P_1 Lagrange finite elements.

Since the Taylor-Flanagan scheme prescribes the contact condition with an implicited Lagrange multiplier and enforces the persistency condition, it is very close to the Paoli-Schatzman scheme with a restitution coefficient $e = 0$ even if the contact condition is prescribed in a slightly different way. The consequence is that the results of the simulations shown on Figure 10 for the Taylor-Flanagan scheme are almost identical to the results shown on Figure 7 for the Paoli-Schatzman scheme with $e = 0$. Particularly, a loss of energy occurs at each impact.

4.1.5 Comparison with the mass redistribution method

The mass redistribution method, introduced in [30], considers a semi-discretization that comes from the finite element approximation of the dynamic contact problem combined with a Lagrange

multiplier method to enforce the contact condition:

$$\mathbf{M}_{\mathrm{r}}\ddot{\mathbf{U}}(t) + \mathbf{K}\mathbf{U}(t) + \mathbf{B}^{\mathrm{T}}\Lambda(t) \ni \mathbf{L}(t), \tag{31}$$

$$\Lambda(t) \leq 0, \quad (\bar{\Lambda} - \Lambda(t))^{\mathrm{T}}\mathbf{B}\mathbf{U}(t) \geq 0, \quad \forall \bar{\Lambda} \leq 0. \tag{32}$$

for a.e. $t \in (0, T]$, still with $\mathbf{K}$ the stiffness matrix, with $\mathbf{B}$ the matrix representing the discrete normal trace operator on the contact boundary, and with $\mathbf{M}_{\mathrm{r}}$ a modified mass matrix with a vanishing contribution on the contact boundary. The matrix $\mathbf{M}_{\mathrm{r}}$ is simply built from the standard mass matrix $\mathbf{M}$ by setting to zero the lines and columns corresponding to the degrees of freedom on the contact boundary and redistributing the removed mass on the internal degrees of freedom (see a possible redistribution algorithm in [30] and other strategies in [17, 26, 55]). In the one-dimensional test–case, this just means setting to zero the first column and first row and adding the removed mass on the first degree of freedom, which as been proved to be the most optimal strategy in [17]. It is proved in [30] that the mass redistribution method allows to recover the well-posedness of the discretization and that the solution to the approximated problem is energy conserving. Some convergence results can be found in [17, 19, 20, 21, 26]. Note also that such singular mass matrices can be obtained with the method introduced in [45] by considering different approximations for the displacement and the velocity instead of using a post-modification of the mass matrix.

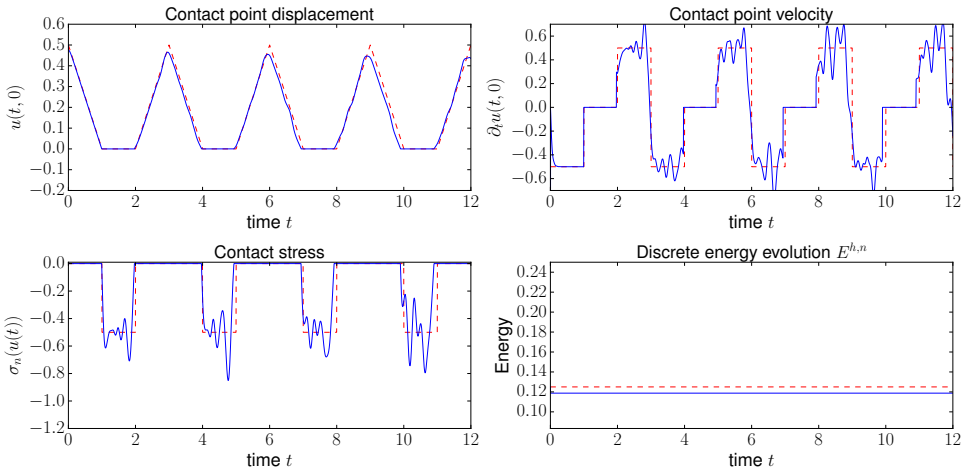

Figure 11: Multiple impacts of an elastic bar. Mass redistribution method for $h = 1/20$, $\tau = 0.01$ and P_1 Lagrange finite elements.

Since the mass matrix admits a kernel containing the vectors being only nonzero on the contact boundary, the system (31)-(32) consists in an algebraic variational inequality when reduced on this kernel. Due to the Lipschitz continuity, with respect to the data, of the solution to this variational inequality, Problem (31)–(32) reduces to a system of ordinary differential equations on the orthogonal of the kernel. This property, detailed in [30] allows to use quite arbitrary time–marching schemes to approximate (31)–(32), among others the Verlet scheme. Of course, the method is not strictly an explicit one since a global solving has to be done on the kernel of the modified mass matrix. However, in the one-dimensional test case, this kernel is one-dimensional which allows an explicit solving.

The corresponding simulations can be seen on Figure 11. One characteristic of the mass redistribution method is to produce low oscillating velocity and contact stress compared to other

discretizations. One can see that the energy is conserved, but slightly modified compared to the standard energy.

4.1.6 Comparison with the penalty method

The penalty method is one of the simplest and most popular way to approximate the contact condition (see for instance [31]). With the notations used to write system (9) for Nitsche's method and with the non-linear operator $\mathbf{B}_{\mathrm{p}}^h : \mathbf{V}^h \to \mathbf{V}^h$, defined for all $\mathbf{v}^h, \mathbf{w}^h \in \mathbf{V}^h$ by

$$(\mathbf{B}_{\mathrm{p}}^h \mathbf{v}^h, \mathbf{w}^h)_{\gamma_h} := a(\mathbf{v}^h, \mathbf{w}^h) + \int_{\Gamma_C} \gamma_h [v_n^h]_{\mathbb{R}^+} w_n^h \, d\Gamma,$$

the dynamic contact problem approximated by a penalty method reads:

$$\begin{cases} \text{Find } \mathbf{u}^h : [0,T] \to \mathbf{V}^h \text{ such that for } t \in [0,T] : \\ \mathbf{M}^h \ddot{\mathbf{u}}^h(t) + \mathbf{B}_{\mathrm{p}}^h \mathbf{u}^h(t) = \mathbf{L}^h(t), \\ \mathbf{u}^h(0,\cdot) = \mathbf{u}_0^h, \qquad \dot{\mathbf{u}}^h(0,\cdot) = \dot{\mathbf{u}}_0^h. \end{cases} \tag{33}$$

This problem corresponds to a nonlinear system of ordinary differential equations on which a Verlet scheme can be applied. The parameter γ_h is now the penalty parameter and, following for instance the analysis in the static case of [10] and similarly to Nitsche's method, we will still consider that $\gamma_h|_{K \cap \Gamma_C} = \gamma_0 / h_K$ for each finite element K.

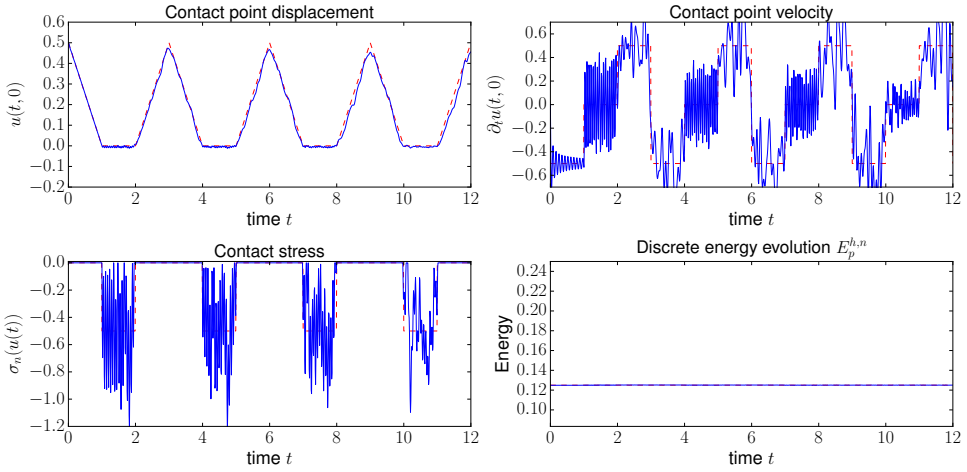

Figure 12: Multiple impacts of an elastic bar. Penalty method for $h = 1/20$, $\tau = 0.01$, $\gamma_0 = 5$ and P_1 Lagrange finite elements.

Figures 12, 13 and 14 depict three simulations for the one-dimensional test case for $\gamma_0 = 5$, $\gamma_0 = 1$ and $\gamma_0 = 0.25$, respectively. The augmented energy associated to penalty is the following one [28]:

$$E_p^{h,n} = E^{h,n} + \frac{1}{2} \int_{\Gamma_C} \gamma_h [v_n^{h,n}]_{\mathbb{R}^+}^2 \, d\Gamma.$$

For $\gamma_0 = 0.25$ the contact interface is clearly too soft and a large penetration occurs, which makes the approximated solution being far from the exact one. Conversely, for $\gamma_0 = 5$, the non-penetration condition is better approximated, but some important oscillations on the velocity of

the contact point and on the contact stress occur. Similarly to Nitsche's method, an acceptable compromise seems to set $\gamma_0 = 1$, which corresponds to comparable stiffnesses on the contact point due to both the penalty term, on one side, and to the interior elasticity terms, on the other.

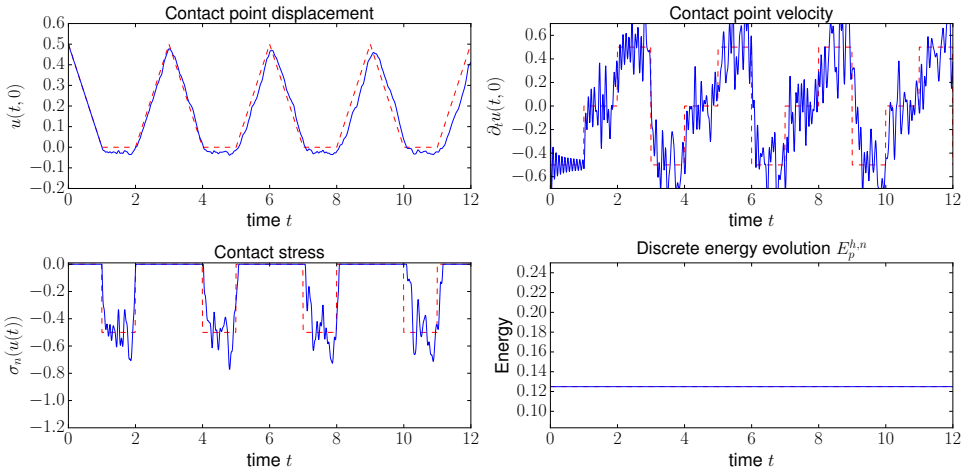

Figure 13: Multiple impacts of an elastic bar. Penalty method for $h = 1/20$, $\tau = 0.01$, $\gamma_0 = 1$ and P_1 Lagrange finite elements.

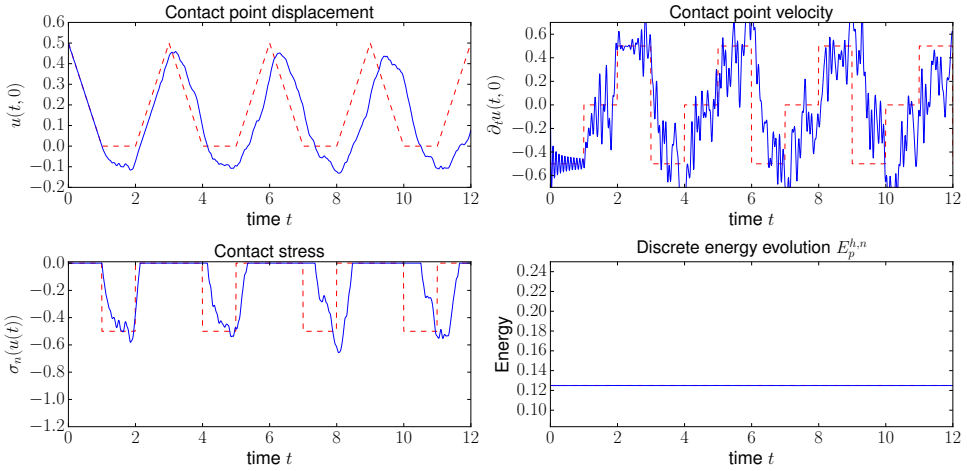

Figure 14: Multiple impacts of an elastic bar. Penalty method for $h = 1/20$, $\tau = 0.01$, $\gamma_0 = 0.25$ and P_1 Lagrange finite elements.

It is worth comparing Figure 13 to Figures 2, 3 and 4 for Nitsche's method and the same value of the parameter γ_0. The non-penetration condition is better satisfied with Nitsche's method, which highlights its consistency. However, energy conservation is better preserved by the penalty method except when the variant $\Theta = 1$ of Nitsche's method is used.

4.1.7 Numerical convergence

Simulations in the previous sections allow a qualitative comparison of the different studied methods on the one-dimensional test–case. The aim of this section is to complete this comparison with

a convergence study, still for the same test–case. This is done for both linear finite elements (P_1 Lagrange) on Figure 15 and quadratic finite elements (P_2 Lagrange) on Figure 16. For M the number of elements, $h = 1/M$ is the element size and the time–step is chosen to be $\tau = h/10$ for P_1 elements and $\tau = h/20$ for P_2 elements.

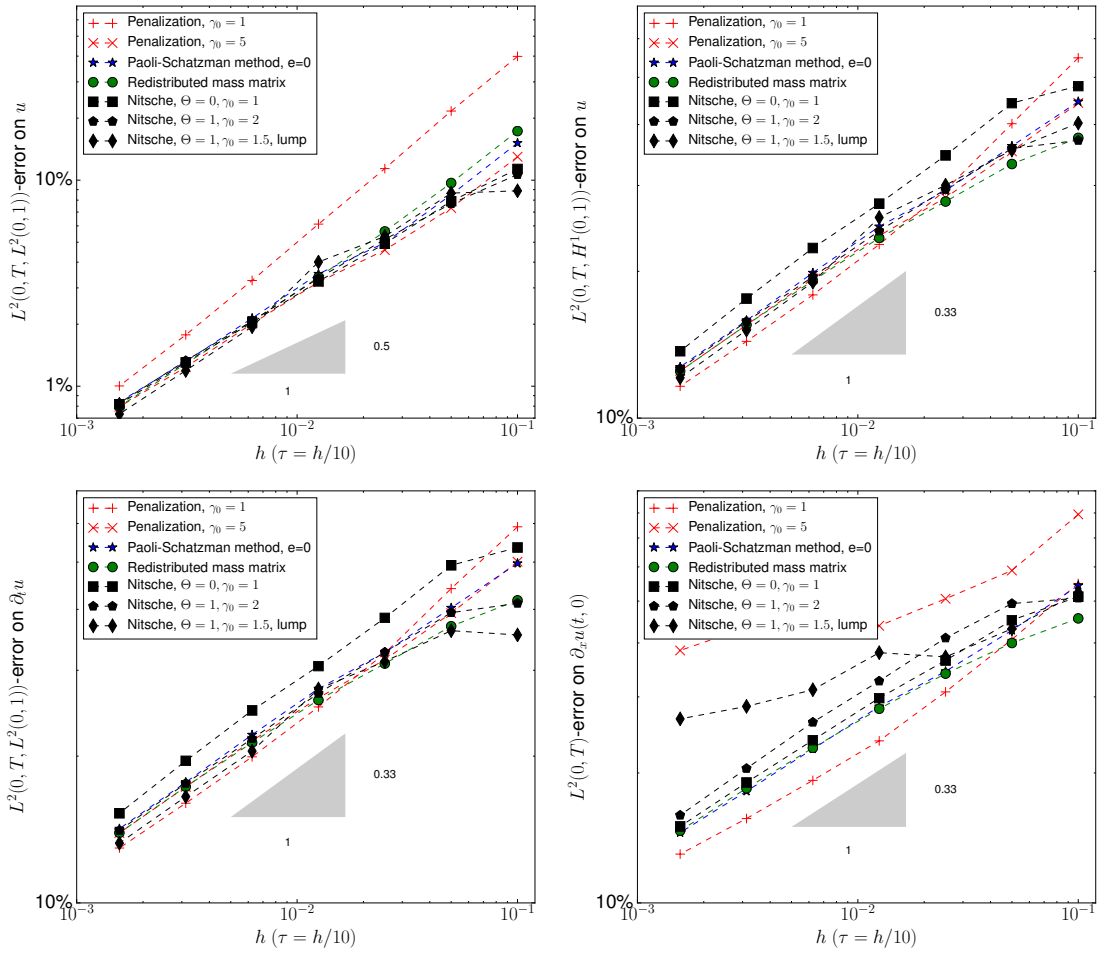

Figure 15: Multiple impacts of an elastic bar. Convergence tests for P_1 Lagrange finite elements.

A comparison of figures 15 and 16 leads to the conclusion that despite the very low regularity of the exact solution (velocity and stress are discontinuous), there is a substantial gain in using quadratic elements. It even improves the convergence rate for the $L^2(0,T,L^2(\Omega))-$norm of the error of the displacement. Globally, the mass redistribution with quadratic elements provides the best compromise. However, as the Paoli-Schatzman scheme, it necessitates to solve a global problem on the contact surface.

So, if we limit the comparison to primal discretizations, which do not require to solve such a global problem (except the inversion of the mass matrix if the mass matrix is not lumped), we can compare only Nitsche and penalty methods. What can be observed, especially on the $L^2(0,T,L^2(\Omega))-$norm of the error in displacement, is that Nitsche's method is less sensitive to the parameter γ_0 due to its consistency. The difficulty to achieve a good compromise for penalty method is illustrated on Figure 15: a low γ_0 allows a good approximation of the contact stress, but the worst approximation of the $L^2(0,T,H^1(\Omega))$-norm of the displacement for coarse meshes.

Conversely, a large γ_0 leads to a better approximation for the $L^2(0,T,H^1(\Omega))$-norm but a too much oscillatory solution which prevents the $L^2(0,T)$ convergence of the contact stress. There is, however, also a constraint for the choice of γ_0 with Nitsche's method because it has to be chosen sufficiently large to preserve the coercivity of the formulation (see Remark 3.6 and Figure 4).

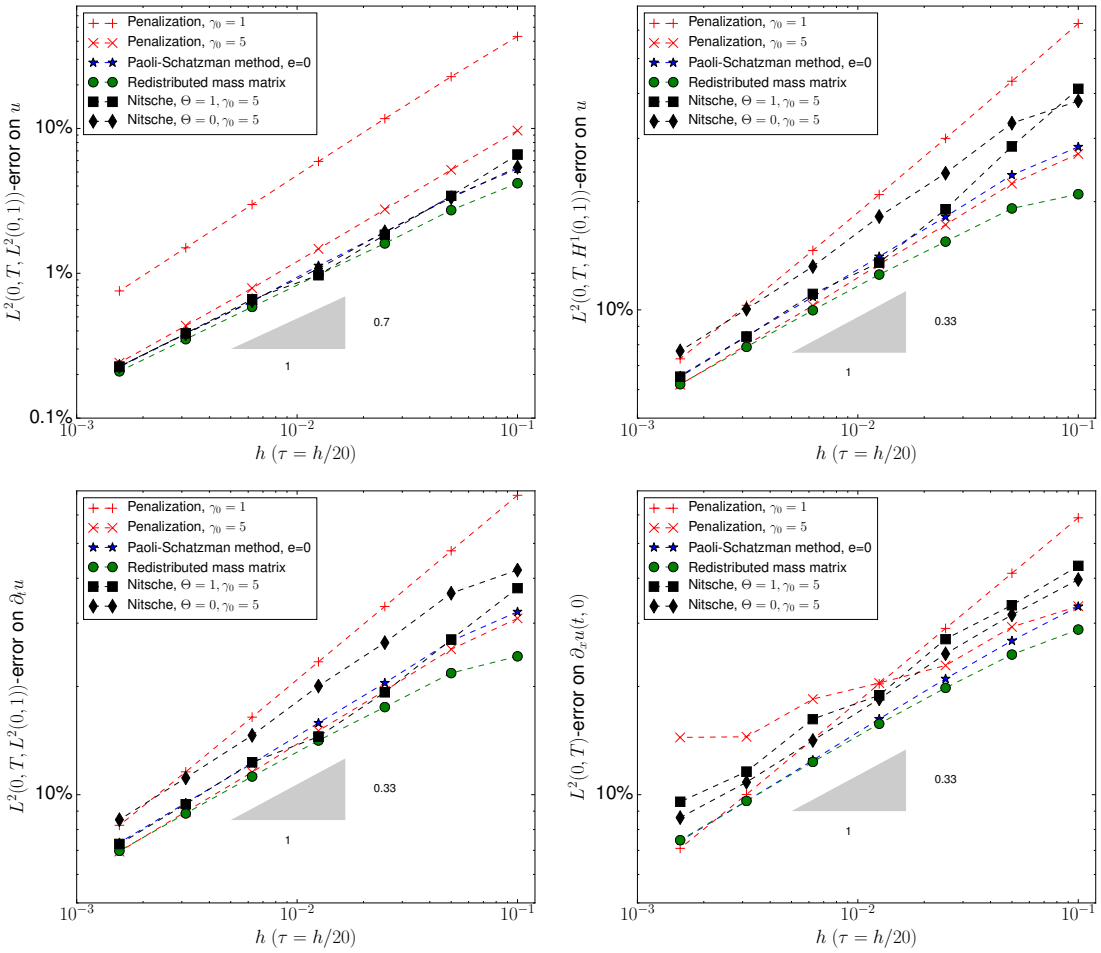

Figure 16: Multiple impacts of an elastic bar. Convergence tests for P_2 Lagrange finite elements.

4.2 2D/3D numerical experiments: multiple impacts of a disc / a sphere

Numerical experiments are then carried out in 2D and 3D, to assess the behavior of Nitsche's method in a more realistic situation. We study the impact of a disc and a sphere on a rigid support. The physical parameters are the following: the diameter of the disc is $D = 40$, the Lamé coefficients are $\lambda = 30$ and $\mu = 30$, and the material density is $\rho = 1$. The total simulation time is $T = 120$.

The volume load in the vertical direction is set to $\|\mathbf{f}\| = 0.1$ (gravity, oriented towards the support). On the upper part of the boundary is applied a homogeneous Neumann condition $\mathbf{g} = \mathbf{0}$ and the lower part of the boundary is the contact zone Γ_C. There an initial vertical displacement ($\mathbf{u}_0 = (0,4)$) and no initial velocity ($\dot{\mathbf{u}}_0 = \mathbf{0}$). In such a situation, there is up to our knowledge no analytic solution to validate the numerical results.

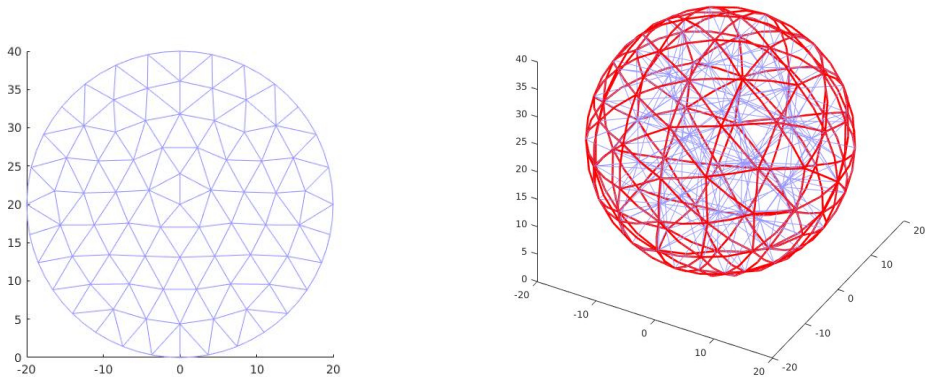

Figure 17: P_2 meshes used for the ball and the sphere.

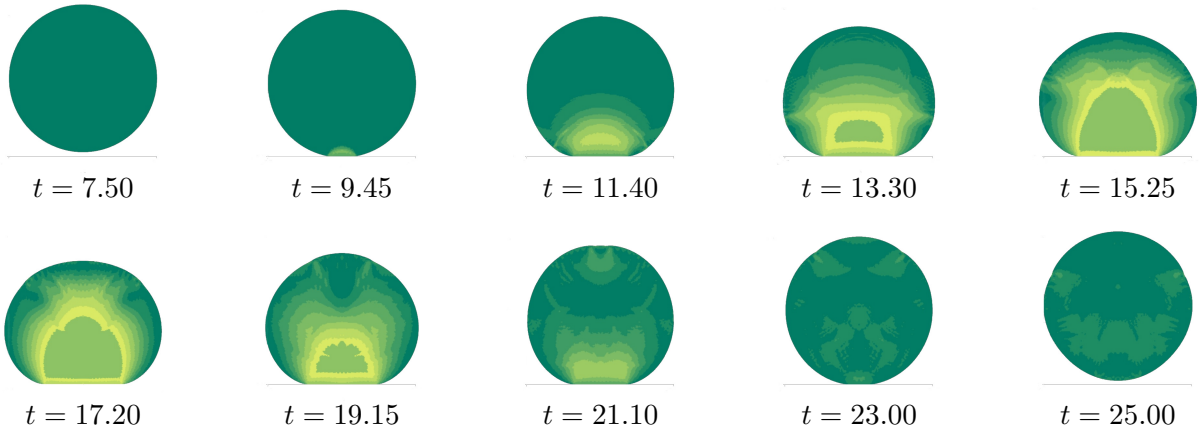

Figure 18: First bounce of the disc. Von Mises stress distribution.

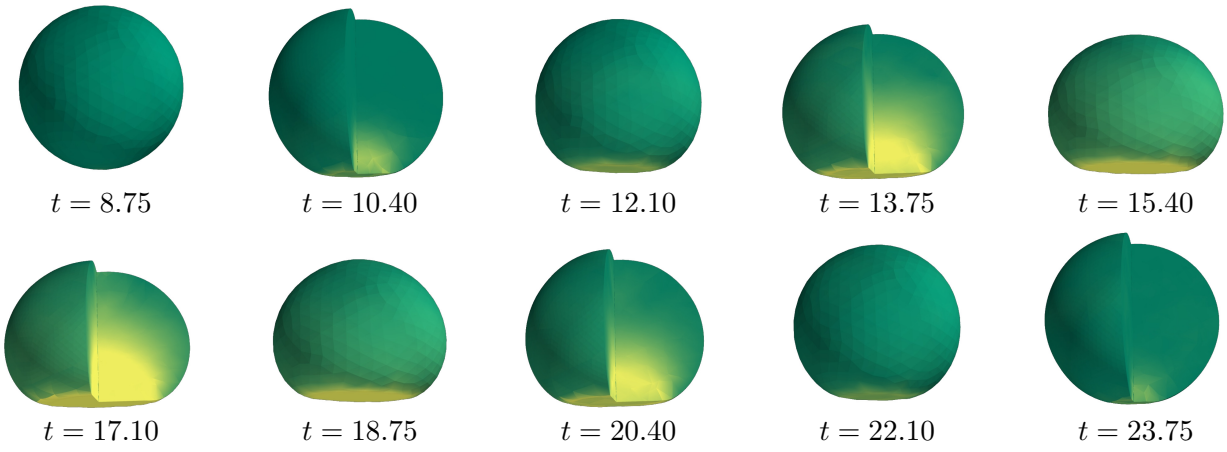

Figure 19: First bounce of the sphere. Von Mises stress distribution. One view over two is a sectional one.

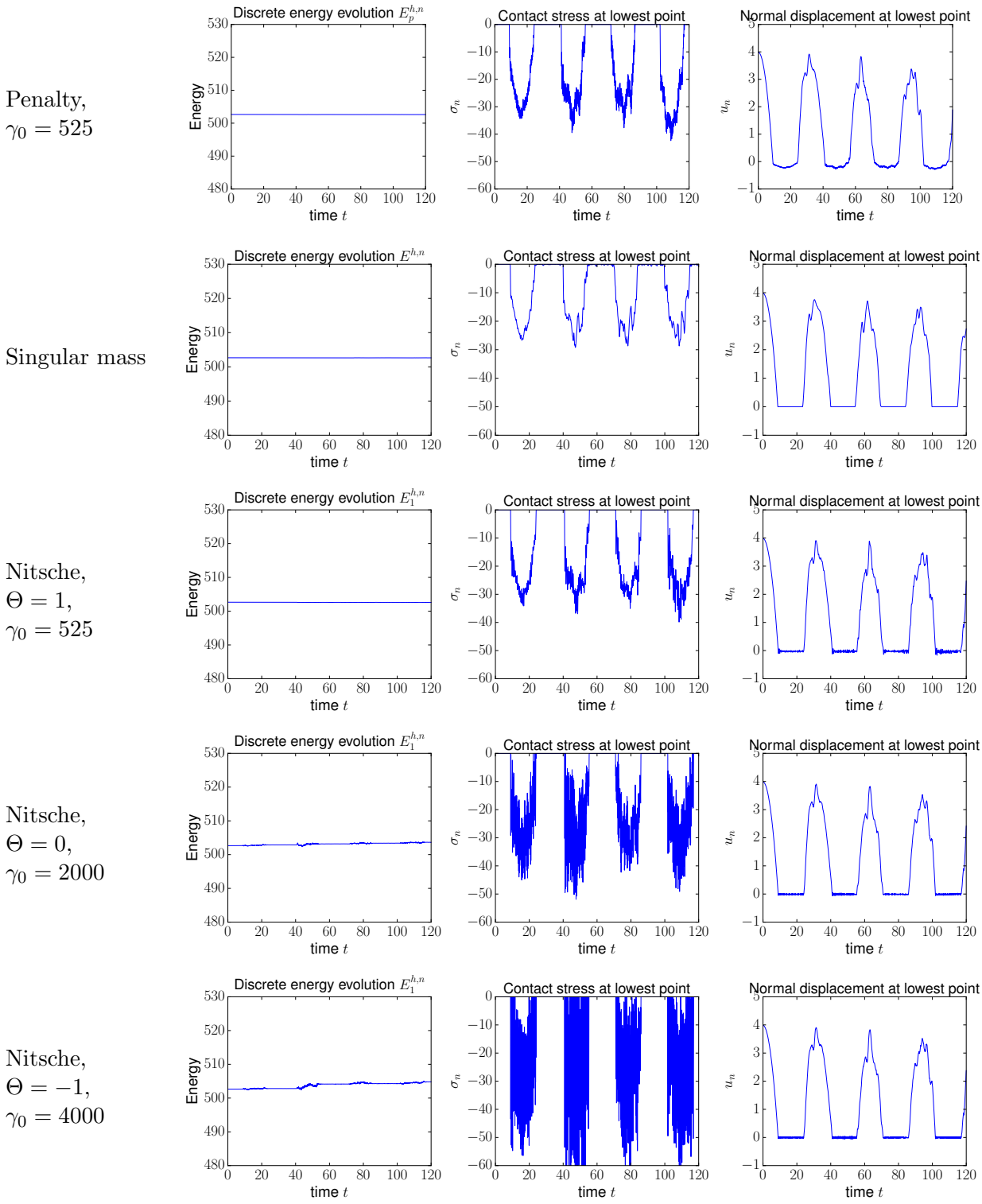

Figure 20: Comparison of the penalty, singular mass and Nitsche methods in the 2D case.

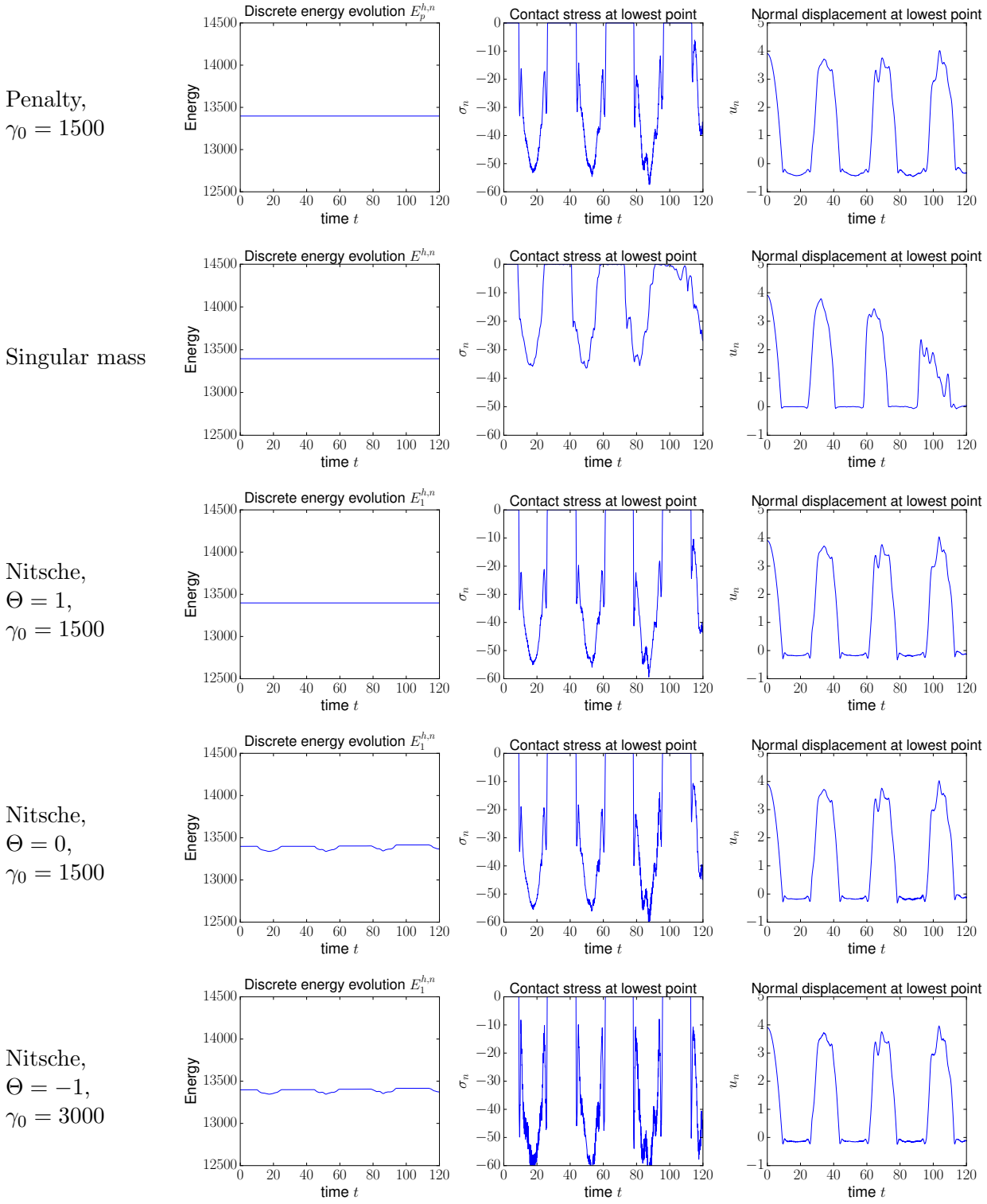

Figure 21: Comparison of the penalty, singular mass and Nitsche methods in the 3D case.

For space semi-discretization, Lagrange isoparametric finite elements of order $k = 2$ have been

used. The mesh size is $h = 4$ for the ball and $h = 8$ for the sphere (see Figure 17). Integrals of the non-linear term on Γ_C are computed with standard quadrature formulas of order 4. A snapshot of the evolution of the disc and the sphere during the first impact can be seen on Figure 18 and Figure 19.

The comparison of the simulations for the different methods is depicted Figure 20 for the two-dimensional case and Figure 21 for the three-dimensional case. For the sake of shortness, only the penalty, the singular mass and Nitsche methods are compared. First of all, a conclusion that can be drawn from these numerical experiments is that the tested methods are all capable of reliably approximating two and three-dimensional dynamic contact problems. An important difference between simulations in dimension 2 and 3 is a much smaller oscillation of the contact stress in dimension 3, except for the mass redistribution method which is not subjected to spurious oscillations. The energy is conserved more strictly with the penalty method, the mass redistribution method and the variant $\Theta = 1$ of Nitsche's method, the other two variants presenting significant disturbances in the energy evolution. The mass redistribution method appears to give the best compromise between energy conservation and the low level of oscillation on the contact boundary. Note however that it produces a weakening of the rebound, mainly in dimension 3, which we do not explain. The lake of consistency of the penalty method is illustrated on the normal displacement graph where we can note a larger interpenetration compared to the other methods. Finally, among the variants of Nitsche's method, the symmetric variant $\Theta = 1$ is the one that achieves the best compromise between energy conservation and the level of oscillations of the contact stress, which remains moderate.

5 Concluding remarks

In this paper, we studied the application of an explicit Verlet scheme for the approximation of elastodynamic contact problems with Nitsche's method. The explicit method being commonly used in elastodynamic contact problems, it seemed important to complete the study that had been performed in [11, 12] for implicit schemes. We tried to characterize the stability properties of the different variants of Nitsche's method for the Verlet scheme and we introduced a number of necessary tools for this analysis. Of course, we are aware that the stability result we establish is very partial (only for $\Theta = 1$) and certainly suboptimal: a stability condition such as $\tau = \mathcal{O}(h)$ would be more satisfactory and would correspond to what we noted in numerical tests. This result remains to be refined. Moreover, it would certainly be possible to prove a convergence result in dimension one, as in [19], because in this context the existence and uniqueness of the solution is theoretically proven. We numerically compared the Nitsche method to the main existing methods that can support an explicit scheme: the Paoli-Schatzman scheme, the Taylor-Flanagan scheme, the mass redistribution method and the penalty method. It should be noted that among these methods, only the penalty method and Nitsche's method support a really explicit resolution since the others incorporate an implicit resolution of the contact force. Finally, among the variants of Nitsche's method, the symmetric variant $\Theta = 1$ seems to be the most suitable for solving dynamic contact problems mainly because of its energy conservation properties. For the other variants a gain of energy can be observed, especially for low values of Nitsche's parameter γ_0. Further study of the effect of the mass matrix lumping, particularly on the stability of the method, and of the proper choice of the Nitsche's parameter γ_0 are some perspectives of this work.

References

[1] R.-A. Adams, *Sobolev spaces*, vol. 65 of Pure and Applied Mathematics, Academic Press, New York-London, 1975.

[2] J. Ahn and D. E. Stewart, *Existence of solutions for a class of impact problems without viscosity*, SIAM J. Math. Anal., 38 (2006), pp. 37–63.

[3] P. Alart and A. Curnier, *A generalized Newton method for contact problems with friction*, J Mec. Theor. Appl., 7 (1988), pp. 67–82.

[4] F. Armero and E. Petőcz, *Formulation and analysis of conserving algorithms for frictionless dynamic contact/impact problems*, Comput. Methods Appl. Mech. Engrg., 158 (1998), pp. 269–300.

[5] T. Belhytschko and M. Neal, *Contact-impact by the pinball algorithm with penaly and lagrangian methods*, Internat. J. Numer. Methods Engrg., 31 (1991), pp. 547–572.

[6] S.-C. Brenner and L.-R. Scott, *The mathematical theory of finite element methods*, vol. 15 of Texts in Applied Mathematics, Springer-Verlag, New York, 2007.

[7] F. Chouly, *An adaptation of Nitsche's method to the Tresca friction problem*, J. Math. Anal. Appl., 411 (2014), pp. 329–339.

[8] F. Chouly, M. Fabre, P. Hild, R. Mlika, J. Pousin, and Y. Renard, *An overview of recent results on Nitsche's method for contact problems*, Lecture Notes in Computational Science and Engineering, 121 (2018), pp. 93–141.

[9] F. Chouly and P. Hild, *A Nitsche-based method for unilateral contact problems: numerical analysis*, SIAM J. Numer. Anal., 51 (2013), pp. 1295–1307.

[10] ——, *On convergence of the penalty method for unilateral contact problems*, Appl. Numer. Math., 65 (2013), pp. 27–40.

[11] F. Chouly, P. Hild, and Y. Renard, *A Nitsche finite element method for dynamic contact: 1. Space semi-discretization and time-marching schemes*, ESAIM Math. Model. Numer. Anal., 49 (2015), pp. 481–502.

[12] ——, *A Nitsche finite element method for dynamic contact: 2. Stability of the schemes and numerical experiments*, ESAIM Math. Model. Numer. Anal., 49 (2015), pp. 503–528.

[13] ——, *Symmetric and non-symmetric variants of Nitsche's method for contact problems in elasticity: theory and numerical experiments*, Math. Comp., 84 (2015), pp. 1089–1112.

[14] P.-G. Ciarlet, *The finite element method for elliptic problems*, vol. II of Handbook of Numerical Analysis (eds. P.G. Ciarlet and J.L. Lions), North-Holland Publishing Co., Amsterdam, 1991.

[15] F. Cirak and M. West, *Decomposition contact response (DCR) for explicit finite element dynamics*, Internat. J. Numer. Methods Engrg., 64 (2005), pp. 1078–1110.

[16] G. Cohen and S. Pernet, *Finite element and discontinuous Galerkin methods for transient wave equations*, Scientific Computation, Springer, Dordrecht, 2017.

[17] F. Dabaghi, P. Krejči, A. Petrov, J. Pousin, and Y. Renard, *A weighted finite element mass redistribution method for dynamic contact problems*, J. Comp. Appl. Math., (to appear).

[18] F. Dabaghi, A. Petrov, J. Pousin, and Y. Renard, *Convergence of mass redistribution method for the one-dimensional wave equation with a unilateral constraint at the boundary*, M2AN Math. Model. Numer. Anal., 48 (2014), pp. 1147–1169.

[19] ——, *A robust finite element redistribution approach for elastodynamic contact problems*, Appl. Numer. Math., 103 (2016), pp. 48–71.

[20] D. Doyen and A. Ern, *Convergence of a space semi-discrete modified mass method for the dynamic Signorini problem*, Commun. Math. Sci., 7 (2009), pp. 1063–1072.

[21] ——, *Analysis of the modified mass method for the dynamic Signorini problem with Coulomb friction*, SIAM J. Numer. Anal., 49 (2011), pp. 2039–2056.

[22] D. Doyen, A. Ern, and S. Piperno, *Time-integration schemes for the finite element dynamic Signorini problem*, SIAM J. Sci. Comput., 33 (2011), pp. 223–249.

[23] ——, *Quasi-explicit time-integration schemes for dynamic fracture with set-valued cohesive zone models*, Comput. Mech., 52 (2013), pp. 401–416.

[24] C. Eck, J. Jarušek, and M. Krbec, *Unilateral contact problems*, vol. 270 of Pure and Applied Mathematics (Boca Raton), Chapman & Hall/CRC, Boca Raton, FL, 2005.

[25] A. Ern and J.-L. Guermond, *Theory and practice of finite elements*, vol. 159 of Applied Mathematical Sciences, Springer-Verlag, New York, 2004.

[26] C. Hager, S. Hüeber, and B. I. Wohlmuth, *A stable energy-conserving approach for frictional contact problems based on quadrature formulas*, Internat. J. Numer. Methods Engrg., 5 (2008), pp. 918–932.

[27] E. Hairer, C. Lubich, and G. Wanner, *Geometric numerical integration*, vol. 31 of Springer Series in Computational Mathematics, Springer-Verlag, Berlin, second ed., 2006. Structure-preserving algorithms for ordinary differential equations.

[28] P. Hauret and P. Le Tallec, *Energy-controlling time integration methods for nonlinear elastodynamics and low-velocity impact*, Comput. Methods Appl. Mech. Engrg., 195 (2006), pp. 4890–4916.

[29] M. Heinstein, F. Mello, S. Attaway, and T. Laursen, *Contact-impact modeling in explicit transient dynamics*, Comput. Methods Appl. Mech. Engrg., 187 (2000), pp. 621–640.

[30] H. B. Khenous, P. Laborde, and Y. Renard, *Mass redistribution method for finite element contact problems in elastodynamics*, Eur. J. Mech. A Solids, 27 (2008), pp. 918–932.

[31] N. Kikuchi and J. T. Oden, *Contact problems in elasticity: a study of variational inequalities and finite element methods*, vol. 8 of SIAM Studies in Applied Mathematics, Society for Industrial and Applied Mathematics (SIAM), Philadelphia, PA, 1988.

[32] J. U. Kim, *A boundary thin obstacle problem for a wave equation*, Comm. Partial Differential Equations, 14 (1989), pp. 1011–1026.

[33] T. A. Laursen and V. Chawla, *Design of energy conserving algorithms for frictionless dynamic contact problems*, Internat. J. Numer. Methods Engrg., 40 (1997), pp. 863–886.

[34] G. Lebeau and M. Schatzman, *A wave problem in a half-space with a unilateral constraint at the boundary*, J. Differential Equations, 53 (1984), pp. 309–361.

[35] J. J. Moreau, *Unilateral contact and dry friction in finite freedom dynamics*, Springer, Vienna, 1988, pp. 1–82.

[36] ——, *Numerical aspects of the sweeping process*, Comput. Methods Appl. Mech. Engrg., 177 (1999), pp. 329–349.

[37] N. M. Newmark, *A method of computation for structural dynamics*, J. Eng. Mech. Div.–ASCE, 85 (1959), pp. 67–94.

[38] J. Nitsche, *Über ein Variationsprinzip zur Lösung von Dirichlet-Problemen bei Verwendung von Teilräumen, die keinen Randbedingungen unterworfen sind*, Abhandlungen aus dem Mathematischen Seminar der Universität Hamburg, 36 (1971), pp. 9–15.

[39] L. Paoli and M. Schatzman, *Schéma numérique pour un modèle de vibrations avec contraintes unilatérales et perte d'énergie aux impacts, en dimension finie*, C. R. Acad. Sci. Paris Sér. I Math., 317 (1993), pp. 211–215.

[40] ——, *Approximation et existence en vibro-impact*, C.R. Acad. Sci. Paris, 329, Série I (1999), pp. 1103–1107.

[41] ——, *A numerical scheme for impact problems. I. The one-dimensional case*, SIAM J. Numer. Anal., 40 (2002), pp. 702–733.

[42] ——, *A numerical scheme for impact problems. II. The multidimensional case*, SIAM J. Numer. Anal., 40 (2002), pp. 734–768.

[43] ——, *Numerical simulation of the dynamics of an impacting bar*, Comput. Methods Appl. Mech. Engrg., 196 (2007), pp. 2839–2851.

[44] C. Pozzolini, Y. Renard, and M. Salaün, *Vibro-impact of a plate on rigid obstacles: existence theorem, convergence of a scheme and numerical simulations*, IMA J. Numer. Anal., 33 (2013), pp. 261–294.

[45] Y. Renard, *The singular dynamic method for constrained second order hyperbolic equations: application to dynamic contact problems*, J. Comput. Appl. Math., 234 (2010), pp. 906–923.

[46] R. A. Ryckman and A. J. Lew, *An explicit asynchronous contact algorithm for elastic body-rigid wall interaction*, Internat. J. Numer. Methods Engrg., 89 (2012), pp. 869–896.

[47] M. Schatzman, *A hyperbolic problem of second order with unilateral constraints: the vibrating string with a concave obstacle*, J. Math. Anal. Appl., 73 (1980), pp. 138–191.

[48] ——, *Un problème hyperbolique du 2ème ordre avec contrainte unilatérale: la corde vibrante avec obstacle ponctuel*, J. Differential Equations, 36 (1980), pp. 295–334.

[49] T. Schindler and V. Acary, *Timestepping schemes for nonsmooth dynamics based on discontinuous Galerkin methods: definition and outlook*, Math. Comput. Simulation, 95 (2014), pp. 180–199.

[50] R. Stenberg, *On some techniques for approximating boundary conditions in the finite element method*, J. Comput. Appl. Math., 63 (1995), pp. 139–148.

[51] J. R. Stewart, A. S. Gullerud, and M. W. Heinstein, *Solution verification for explicit transient dynamics problems in the presence of hourglass and contact forces*, Comput. Methods Appl. Mech. Engrg., 195 (2006), pp. 1499–1516.

[52] L. Taylor and D. Flanagan, *PRONTO3D: A three-dimensionnal transient solid dynamics program, SAND89-1912*, 1989.

[53] V. Thomée, *Galerkin finite element methods for parabolic problems*, vol. 25 of Springer Series in Computational Mathematics, Springer-Verlag, Berlin, 1997.

[54] D. Vola, M. Raous, and J. A. C. Martins, *Friction and instability of steady sliding: squeal of a rubber/glass contact*, Internat. J. Numer. Methods Engrg., 46 (1999), pp. 1699–1720.

[55] B. I. Wohlmuth, *Variationally consistent discretization schemes and numerical algorithms for contact problems*, Acta Numer., 20 (2011), pp. 569–734.

[56] S. Wolff and C. Bucher, *Asynchronous collision integrators: explicit treatment of unilateral contact with friction and nodal restraints*, Internat. J. Numer. Methods Engrg., 95 (2013), pp. 562–586.